

SEMI-ANNUAL REPORT

X-RAYS FROM FISSION

Sponsored by

ADVANCED RESEARCH PROJECTS AGENCY

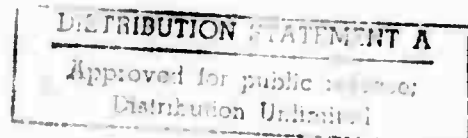
Form Approved Budget Bureau No. 22-R0293



AD 749402

Program Code Number	OF10
ARPA Order Number	1571
Name of Contractor	The University of Texas at Austin
Date of Contract	1 April 1972
Contract Number	N00014-67-A-0126-0012
Amount of Contract	\$167,505.00
Contract Expiration Date	31 December 1972
Short Title of Work	X-Rays from Fission
Principal Investigators	C. Fred Moore, Professor of Physics G. W. Hoffmann, Assistant Professor of Physics

Reproduced by  
NATIONAL TECHNICAL  
INFORMATION SERVICE  
U S Department of Commerce  
Springfield VA 22151



**Disclaimer:** The views and conclusions contained in this document are those of the authors and should not be interpreted as necessarily representing the official policies, either expressed or implied, of the Advanced Research Projects Agency or the U. S. Government.

**BEST  
AVAILABLE COPY**

## TABLE OF CONTENTS

	Page
I. INTRODUCTION.....	1
II. FISSION FRAGMENT TIME-OF-FLIGHT.....	2
III. TIME-OF-FLIGHT-ENERGY-X-RAY COINCIDENCE MEASUREMENTS FOR THE DETERMINATION OF ISOTOPIC FISSION YIELDS.....	5
IV. NEUTRON-INDUCED FISSION.....	8
V. PUBLICATIONS SINCE LAST REPORT.....	9
VI. RECENT BIBLIOGRAPHY.....	10
VII. WORK STATEMENT.....	12
VIII. PERSONNEL.....	13
APPENDIX	

## I A INTRODUCTION

This is a report on the activities pursued during the first six months of the third year contract "X-Rays from Fission." The main effort during this part of the contract has been the construction and testing of a time-of-flight tube and the testing of the associated electronics and detectors. Much of the effort during the previous two contract years has been to study fission yields from experiments in which fragment mass was not determined directly. These experiments involved coincidence measurements between X-rays and/or  $\gamma$ -rays. During the course of these experiments it was found that the K-X-rays and  $\gamma$ -rays emitted at the time of fission come primarily from nuclear, rather than atomic, processes. Since nuclear properties vary in no systematic fashion from one nucleus to another, these types of experiments are not now being pursued because the extraction of fission isotopic yields from such experiments appears to be in the distant future.

Since it now seems promising that isotopic fission yields can be extracted almost directly from the raw data of energy-time-of-flight-induced L-X-ray coincidence experiments, almost all the present effort is being devoted to these experiments.

## II. FISSION FRAGMENT TIME-OF-FLIGHT

Post-neutron mass distributions (for binary or tertiary fission) can be determined by measuring the time-of-flight of one fragment over some distance and its kinetic energy. As discussed in the previous Annual Report, in order to obtain a mass resolution of 1u. (FWHM) so that the integral nuclear mass distribution (i.e., quantized A yields) may be unfolded from the experimental mass spectrum with a great degree of certainty, one needs a long flight path (of the order of 10m) and a large solid angle (of the order of 5 msr). However, a 10m flight path implies a vanishingly small solid angle ( $4 \times 10^{-2}$  msr for a  $300 \text{ mm}^2$  detector). Oakey and MacFarlane (Nucl. Instru. & Meth., 49 (1967) 220) have shown that this problem can be overcome by using an electrostatic particle guide. Such a guide, which consists of a wire at a negative high voltage running down the center of a cylinder the length of the flight path, allows electrostatic focusing of charged particles - the ions emitted in an angular range of the order of  $2^\circ$  are confined to trajectories around the central wire as they traverse the guide. The collection efficiency of such an electrostatic particle guide is proportional to the ionic charge and the voltage on the wire and inversely proportional to the fragment energy (see the calculations in the previous Annual Report, for example).

As reported in the last Annual Report, an electrostatic particle guide of the above type was constructed at The University of Texas Center

for Nuclear Studies. It consisted of a 10 meter long stainless steel tube with an inside diameter of 5.05 cm and had a 5 mil wire running its length. Initial measurements with this guide indicated that the "effective" solid angle over the 10m flight path was increased by many orders of magnitude as suggested by the calculations. However, experience with this guide showed that the detector had to be located some distance from and shielded from the central wire because of the negative voltage on the wire.

A new particle guide with modifications to avoid the above mentioned problem has now been constructed. The new guide consists of two 10m long, concentric, stainless steel tubes with inside diameters of 4 and 1.7 in. The inner tube is maintained at a high positive voltage and has a 20 mil wire at ground potential running its length. The thicker central wire permits better positioning and experiences fewer problems caused by vibrations of the wire in the potential field. This new guide has been tested and found to perform satisfactorily and in the same manner as the previous guide. A 1m extension has recently been added to the target end of the particle guide so that the second fragment detector will not be in a high neutron flux when neutron induced fission studies are done.

Various simple timing and coincidence experiments have been done with the 10m electrostatic particle guide and a  $^{252}\text{Cf}$  source in order to test the performance of the guide, the electronics and the detectors. A variety of detectors have been tried and promising results with good resolution have been obtained using an ORTEC 130 fission-fragment detector.

Final tests and the performance of experiments are being temporarily held up by two small problems. The present  $^{252}\text{Cf}$  is broken and folded over and as a result emits very few fission fragments along the axis of the guide. A new source is on order and should arrive shortly. When detectors are removed from the guide after performing tests, they have been covered with oil. This oil will, of course, degrade the performance of the detector. Several heating strips have been ordered and will be wrapped around the particle guide. It is hoped that baking out the guide in this manner will remove the oil problem. If this does not eliminate the problem, it may be necessary to replace the present oil roughing pump.

### III. TIME-OF-FLIGHT-ENERGY-X-RAY COINCIDENCE MEASUREMENTS FOR THE DETERMINATION OF ISOTOPIC FISSION YIELDS

Time-of-flight-energy measurements only allow mass determination. In order to obtain isotopic fission yields both charge and mass must be determined simultaneously. Direct physical techniques usually involve measuring in coincidence, at the time of fission, parameters from which Z and A can be determined. With present day resolution in photon spectroscopy, any characteristic X-rays emitted from the fission fragments may be experimentally observed to unambiguously identify the nuclear charge of these fragments. Such observations will only identify particular fission fragment elements and no statements about elemental yields may be made unless the origin(s) of these observed X-rays are known.

A seemingly appropriate technique to determine nuclear charge, in which X-rays associated with the fission fragments are observed and the origin of the X-rays is well understood, has been tested at the Center for Nuclear Studies. This technique is to create vacancies in the electron shells of the fragments by a known atomic process and observe the fluorescence yields (the probability that a vacancy in a given shell results in a radiative transition). Since the fluorescence yields have been measured experimentally and are understood theoretically, extraction of fission charge and isotope yields should be straight-forward. The electron vacancies may be created by allowing the fission fragments to pass through a thin foil (such as carbon). The X-rays resulting from electron transitions may be observed with a high

resolution photon detector situated near the foil. An experiment was performed in which fission fragments were detected in coincidence with X-rays produced when the fragments passed through a thin carbon foil. It was observed that two groups of L X-rays (corresponding to the light and heavy fragments) were produced. The resolution was not good enough (due to the rather poor detector used) to resolve individual lines, but the peaks were located in the energy region where the L X-rays were expected to appear. Thus, this technique seems to work as expected and the technology seems to be at hand to determine fission yields with a very reliable method.

In the last Annual Report a possible triple coincidence experiment using the time-of-flight-energy-X-ray techniques to measure fission isotopic yields was presented. In this experiment the fissioning source was placed at one end of the particle guide with a fission fragment detector placed on line with the center of the guide behind the source. Another fission fragment detector was placed at the other end of the 10m guide. A thin carbon foil was placed in front of this detector and observed by a high resolution photon detector. The fragment detector near the source provided the start pulse and the other fragment detector provided the stop pulse for the time-of-flight measurement. The electronics were arranged to require a triple coincidence between the pulses in both fragment detectors and the pulse in the X-ray detector.

Two modifications to the above triple coincidence experiment are needed and both are allowed by the 1m extension which has been added

to the 10m electrostatic particle guide. The placing of the carbon foil in front of the fragment detector located 10m from the source removes the X-ray detector from the vicinity of high neutron fluxes but also causes an energy uncertainty in the fragments reaching the fragment detector. Since this energy is an important parameter in the experiment, it is necessary to have the best energy resolution possible. Since high neutron fluxes will also degrade the performance of the fragment detectors, the second fragment detector should be moved from the vicinity of the target. Now that the 1m extension has been added to the particle guide, the second fragment detector can be placed 1m from the source and the carbon foil can be placed in front of this fragment detector since an accurate measurement of the energy of the second fission fragment is not necessary.

The above modifications in the placement of the detectors may necessitate modifications in the triple coincidence circuitry given in the last Annual Report. However, computer studies are now underway to determine if the same basic circuitry can be used and corrections can be made by the use of kinematic calculations made by the computer without degrading the energy resolution.

#### IV. NEUTRON-INDUCED FISSION

The goal of this project is to study neutron-induced fission isotopic yields. Before these studies can be undertaken the experimental techniques discussed in Sections II and III must be tested and proven out using a  $^{252}\text{Cf}$  source. If these techniques work, the basic problem standing in the way of neutron-induced studies is that of the neutron source. A Texas Nuclear neutron generator is in the process of being reconditioned. This reconditioning process is requiring much effort and time which could be expended on more crucial phases of this project. We are also looking into the possibilities of updating this generator and of obtaining a large  $^{252}\text{Cf}$  source to use as a neutron source. Modifications of the target chamber of the electrostatic particle guide to accommodate a neutron source must wait until it has been determined what type of neutron source will be used.

## V. PUBLICATIONS SINCE LAST REPORT

1. F. F. Hopkins, J. R. White, C. Fred Moore, and Patrick Richard,  
"Gamma Cascades in  $^{252}\text{Cf}$  Spontaneous Fission Fragments," submitted  
to Physics Rev. C.

## VI. RECENT BIBLIOGRAPHY

1. "Independent Yields of Krypton and Xenon Isotopes in Thermal-Neutron Fission of  $^{235}\text{U}$ . Observation of an Odd-Even Effect in the Element Yield Distribution," B. Ehrenberg and S. Aniel, *Phys. Rev. C* 6 (1972) 619.
2. "Angular Momentum of Primary Products Formed in the Spontaneous Fission of  $^{252}\text{Cf}$ ," J. B. Wilhelmy, E. Cheifety, R. C. Jared, S. G. Thompson, and H. R. Bowman, *Phys. Rev. C* 5 (1972) 2041.
3. "Angular Distribution of Alpha Particles Emitted in the Fission of  $^{252}\text{Cf}$ ," M. Rajagopalan and T. D. Thomas, *Phys. Rev. C* 5 (1972) 2064.
4. "Distribution of Mass in the Spontaneous Fission of  $^{256}\text{Fm}$ ," K. F. Flynn, E. P. Horvitz, C. A. A. Bloomquist, R. P. Barnes, R. K. Sjohlon, P. R. Fields, and L. E. Glendenin, *Phys. Rev. C* 5 (1972) 1725.
5. "Neutron Evaporation and Energy Distribution in Individual Fission Fragments," M. R. Iyer and A. K. Ganguly, *Phys. Rev. C* 5 (1972) 1410.
6. "Gamma-Neutron Competition in the De-Excitation Mechanism of the Fission Fragments of  $^{252}\text{Cf}$ ," H. Nifenecker, C. Signarbieux, M. Ribrag, J. Poitou, and J. Matuszek, *Nucl. Phys.* A189 (1972) 285.
7. "Inner-Shell Ionization of Fission Products During Nuclear Fission," J. V. Noble, *Nucl. Phys.* A187 (1972) 568.
8. "Search for Conversion Electrons Populating the  $^{236}\text{U}$  Fission Isomer," E. Konecny, H. J. Specht, J. Weber, H. Weigmann, R. L. Ferguson, P. Osterman, M. Waldschmidt, and G. Siegert, *Nucl. Phys.* A187 (1972) 426.

9. "Fission Properties of Heavy and Superheavy Nuclei," H. W. Schmitt and U. Mosel, Nucl. Phys. A186 (1972) 1.
10. "A Single-Particle Model Calculation of Total Energy Surfaces in Heavy Nuclei," David E. Maharry and J. P. Davidson, Nucl. Phys. A183 (1977) 371.
11. "Noncharacteristic X-ray Bands Produced in Targets of C, Al, Si, and Solid Ar by Argon Ions at keV Energies," James R. Macdonald and Matt D. Brown, Phys. Rev. Letts. 29 (1972) 4.
12. "Asymmetric Fission in the Two-Center Model," M. G. Mustafa, U. Mosel and H. W. Schmitt, Phys. Rev. Letts. 28 (1972) 1536.
13. "Metastable X-ray Emitters Produced in Beam-Foil Excitation of Fast Chlorine Beams," C. L. Cocke, Basil Curnutte, and J. R. Macdonald, Phys. Rev. Letts. 28 (1972) 1233.
14. "Lifetime Estimates for Asymmetric Fission of  $^{240}\text{Pu}$ , Including Shell Effects," T. Ledergerber and H. C. Pauli, Phys. Letts. 39B (1972) 307.
15. "On a Correlation Between the Properties of Low Lying Collective Levels and Fission Process Observables in Even Nuclei," A. P. Budnik and N. S. Rabotnov, Phys. Letts. 39B (1972) 311.
16. "Total Spontaneous and Isomer Fission Half-Lives of  $^{234}\text{U}$ ,  $^{236}\text{U}$ , and  $^{240}\text{Pu}$ ," M. A. Hooshyar and F. B. Malik, Phys. Letts. 38B (1972) 495.
17. "Effects of  $\text{UO}_2$  Deposit Thickness on Fission-Fragment Double-Kinetic-Energy Measurements," R. A. Lerche, B. W. Wehring, and M. E. Wyman, Nucl. Instru. & Meth. 101 (1972) 287.
18. "Fission Fragment Energy Loss and Spectrum Parameter Changes for  $^{252}\text{Cf}$  Sources Overcoated with Carbon and Gold," H. L. Adair, Nucl. Instru. & Meth. 100 (1972) 467.

## VII. WORK STATEMENT FOR ARPA PROPOSAL

The contractor shall conduct research involving the measurement of prompt fission processes. This research shall include, but not necessarily be limited to the following:

- A. Studies of the spontaneous fission of  $^{252}\text{Cf}$  employing various combinations of multi-parameter coincidence experiments. Parameters may include fission fragment, X-ray, alpha particle, gamma ray, time-of-flight, and neutron.
- B. Studies of neutron induced fission of  $^{235,238}\text{U}$  and  $^{239}\text{Pu}$  employing various combinations of multiple parameter coincidence experiments described above, less the alpha particle measurements.
- C. From an analysis of the above measurements begin a compilation of the total chain yield and the prompt isotopic yield ratios for fission of  $^{235,238}\text{U}$  and  $^{239}\text{Pu}$  as a function of neutron energy. Give priority to  $^{235}\text{U}$  and  $^{239}\text{Pu}$  fission mass distribution resulting from fission spectrum and 14 MeV neutrons.

## VIII. PERSONNEL

1 April 1972 to 30 September 1972

## (a) NUCLEAR SCIENTISTS

C. Fred Moore, Professor (5 Mo. <sup>*</sup> )	6 mo.
Patrick Richard, Associate Professor (4 Mo. <sup>*</sup> )	5 mo.
Gerald Hoffmann, Research Scientist Assoc. III (1 Mo. <sup>*</sup> )	6 mo.
Larry L. Lynn, Research Scientist Associate III	1 mo.

## (b) PRE-DOCTORAL APPOINTMENTS (GRADUATE STUDENTS)

John <del>M.</del> White, Research Assistant I	6 mo.
Forrest Hopkins, Research Assistant II	2 mo.

## (c) ENGINEERING/TECHNICAL STAFF

Mary George, Administrative Clerk (6 Mo. <sup>*</sup> )	6 mo.
Bonnie Wolf, Secretary (6 Mo. <sup>*</sup> )	6 mo.
J. P. Coose, Technical Assistant II	6 mo.
Kenric Speed, Laboratory Assistant II	3½ mo.
Hunter Ellinger, Computer Programmer I (6 Mo. <sup>*</sup> )	6 mo.
A. L. Mitchell, Research Engineer III (6 Mo. <sup>*</sup> )	6 mo.

## (d) LABORATORY STAFF (UNDERGRADUATE STUDENTS)

Roger Jordan, Laboratory Assistant I	3 mo.
Claude Camp, Laboratory Assistant II	5 mo.
Jeffry Fitch, Laboratory Assistant II	5 mo.
Robert Hooks, Laboratory Assistant I	5 mo.
Gary Jacobs, Laboratory Assistant II	1 mo.

\* At no pay

APPENDIX

GAMMA CASCADES IN  $^{252}\text{Cf}$  SPONTANEOUS FISSION FRAGMENTS\*

F. F. Hopkins,<sup>+</sup> J. R. White, C. Fred Moore, and Patrick Richard<sup>†</sup>

Center for Nuclear Studies

University of Texas, Austin, Texas 78712

ABSTRACT

A  $\gamma$ -ray -  $\gamma$ -ray coincidence experiment to measure transitions in the spontaneous fission fragments of  $^{252}\text{Cf}$  has been performed with a 0.14 cc Ge(Li) detector (FWHM 600 eV at 81 keV) and a 40 cc Ge(Li) detector (FWHM 2.8 keV at 1.33 MeV) in close geometry and repeated in an extended geometry involving shielding of one of the prompt fragments. Several low energy cascades have been detected which were previously unreported. In addition partial decay schemes for four of the products,  $^{105}\text{Mo}$ ,  $^{109}\text{Ru}$ ,  $^{111}\text{Ru}$ , and  $^{146}\text{La}$ , have been suggested.

## I. Introduction

The natures of the level schemes of odd  $Z$  and odd  $A$  fragments from the spontaneous fission of  $^{252}\text{Cf}$  have remained for the most part a mystery. Their elucidation has been a challenging experimental problem. Lack of intensity of many of the  $\gamma$ -transitions has prevented an investigation as complete as that obtained for the even-even fission products.<sup>1,2)</sup>  $\gamma$ -rays emitted by certain isotopes populated strongly in the various  $\beta$ -decay processes following both spontaneous fission of  $^{252}\text{Cf}$  and neutron-induced fission of the uranium isotopes have been observed in detail.<sup>3-10)</sup> Presented in this work are the results of two  $\gamma$ - $\gamma$  coincidence experiments, one performed in close and one in extended geometry, which have shed considerable light on certain of the nuclei which have so far escaped a consistent analysis. This experiment, relying heavily on previous assignments of a multitude of transitions in the energy range 45 to 200 keV by X-ray -  $\gamma$ -ray coincidence techniques<sup>11,12)</sup> and higher energy transitions from various sources, was made possible by the excellent resolution furnished by a  $\text{Ge(Li)}$  crystal of 0.14 cc volume. The data indicate certain strong cascades and rudimentary energy level schemes for several of the products expected to be populated directly and by  $\beta$ -decay. Also questions pertaining to previous isotope assignments in the X-ray -  $\gamma$ -ray experiments have been answered to some extent.

## II. Experimental Setup

### A. Close Geometry

A 0.1  $\mu\text{g}$   $^{252}\text{Cf}$  source between two 1/2 mil disks of beryllium was placed directly on the beryllium window of a 0.14 cc Ge(Li) detector. The Be cover stopped the fragments and removed Doppler distortions for any transition longer than about a picosecond. A 40 cc Ge(Li) detector was placed approximately 3/4" from the source, at which distance the singles count rate was 10,000 counts/sec. The count rate in the smaller crystal was 5,000 counts/sec. At these rates the respective resolutions were 2.8 keV FWHM at 1.33 MeV and 600 eV FWHM at 81 keV. The timing and linear signals were routed through the circuitry shown in Fig. 1. With a timing window of about 150 nanosec, a coincidence count rate estimated at 100/sec was encountered. The logic signal accompanied by the two linear signals was accepted by a computer program which performed a sort of the  $\gamma$ -rays from the 40 cc crystal according to windows set on the peaks in the spectrum from the 0.14 cc detector. All processing was done online. In this way 1K spectra were built of  $\gamma$ -rays from 45 keV to 1300 keV in coincidence with the many lines in the energy range 45 - 200 keV. In the following discussion, figures, and tables, these are the data referred to unless otherwise specified.

Calibrations were taken daily in both detectors with standard sources. A run of 7 days was made. During that time no adjustments had to be made on the gates. Also no gain drift for the electronics associated with the 40 cc counter was found.

### B. Extended Geometry (EG)

An additional experiment was performed in order to help remove some of the ambiguity involved in identification of the  $\gamma$ -lines in the previously described spectra, i.e. the fact that  $\gamma$ -rays both from the nucleus supplying the gate  $\gamma$ -ray and from its possible complementary nuclei arising from the binary fission event will show up in those sorted spectra. A  $^{252}\text{Cf}$  source mounted on a thick copper foil was positioned as shown in Fig. 2. The open-faced side of the source pointed back into a lead shield which afforded a  $3/4$ " thick lead shield between the fragments in flight and the 0.14 cc Ge(Li) detector. Approximately  $1\ 1/2$ " of lead separated the fragments from a 30 cc Ge(Li) detector. In this way  $\gamma$ -rays emitted more than about 1 nanosec after fission were substantially attenuated, especially the low energy lines which were of special interest in this experiment. In a binary event one of the fragments would be stopped in the copper foil while the other would be localized within the shielding apparatus. Those  $\gamma$ -rays emitted by fragments in flight within times of less than a nanosec--that is, those given off while the moving fragment was still visible to the detectors--would be greatly Doppler broadened due to the isotropy of the fragment emission. The intent in this procedure was to isolate cascades in the stopped fragments by gating on non-distorted peaks in the spectrum from the 0.14 cc crystal and separating out coincident non-distorted  $\gamma$ -rays in the 30 cc detector. Certainly a given gate in the low-energy spectrum might include some parts of tails of neighboring distorted peaks, but the low-energy lines considered with successively longer lifetimes for higher

multipolarities starting with E1, M1, etc., this interference would be minimal. Strong effects, i.e. coincidences in the stopped nuclei, should predominate in the data.

The count rate for the 0.14 cc detector was 600/sec while that for the 30 cc detector was around 2000. The respective resolutions were 500 eV FWHM at 81 keV and 3.5 keV FWHM at 356 keV. The electronics was identical to that for the close-geometry experiment. The coincidence rate was about 3/sec. In this case, however, the data was stored event by event as 8K values on magnetic tape. Actual running time was about 6 weeks. Calibrations were taken daily. The data was analyzed offline in a fashion similar to that described above. The gating was done on an 8K spectrum from the smaller detector and the sorted spectra from the 30 cc detector were reduced to 1K. Gate adjustments were required several times through the course of reduction. The gain for the larger detector varied no more than 0.2 channel from the original value up to channel 300, which included all of the data presented in this paper; as a consequence, the sorted spectra, reduced approximately two days worth at a time ( $\sim 500,000$  coincidence events), were simply accumulated with no computer adjustments.

### III. Results

The total coincidence spectrum from the 0.14 cc detector for a 36 hour run in the close geometry experiment is presented in Fig. 3. The statistical clarity of the peaks ranges from excellent to poor in less

intense cases. Gates were set on the gamma rays appearing in Table I. In a few cases two gates were set on a broader than ordinary peak to check for unresolved lines. The background is mostly Compton scattering of higher energy  $\gamma$ -rays. The photopeak-to-associated-Compton ratio for these low energy lines was very high, as expected, since gates seldom showed any  $\gamma$ -rays associated with the appropriate neighboring peaks. The low-energy portion of the total coincidence spectrum from the 40 cc detector, the only part with any number of distinguishable lines, is presented in Fig. 4. These strong lines were noticeable as background in all of the sorted spectra.

The spectra from the shielded detectors run were similar but had worse statistics due to the geometry. The lower energy spectrum is in Fig. 5. Except for three large Pb X-ray peaks arising from  $\gamma$ -fluorescence, it is almost identical to the one in Fig. 3. As expected, Doppler effects do not appear to any large extent and most of the spectrum can be assumed to have come from fragments stopped in the copper foil.

The completeness of and the confidence in the assignments of the  $\gamma$ -cascades in this data varied tremendously from line to line. As stated before, one of the primary means of locating a suspected cascade was to check for identity of the low-energy  $\gamma$ -ray gated on from previous work. A low-energy  $\gamma$ -ray in coincidence with another low-energy line in either the same or a complementary nucleus should have been recorded in the X-ray -  $\gamma$ -ray data, as the high internal conversion probability associated with the second transition should result in a high X-ray

production and therefore high detection probability. In the first case the  $\gamma$ -ray would be noticed in a gate on an X-ray from the same nucleus and perhaps in a gate on a complementary X-ray, depending on the internal conversion probabilities of the complementary nuclei; in the second the  $\gamma$ -ray would be seen at least in a gate on the "complementary" X-ray. In several instances a given gate was within 0.2 keV of more than one line recorded in the X-ray -  $\gamma$ -ray data. The resulting sorted spectra were simply treated as possible combinations of lines associated with each.

There is, in an analysis of this type, a measure of uncertainty introduced by the difference in the means of detection. A  $\gamma$ -ray in the total coincidence spectrum of the  $\gamma$ - $\gamma$  experiment would not necessarily have been recorded by the X-ray -  $\gamma$ -ray work if, for example, it was primarily in coincidence with a high energy transition. However  $\gamma$ -rays of every energy gated on, in Table I, were seen in at least one X-ray gate and most of them strongly. The key is identification of the  $\gamma$ -rays in the gated spectrum from previous work. The shielded data served as a check on some of the stronger cascades.

Once known lines are picked out and thereby verified to be in cascade with the gate  $\gamma$ -ray, the remaining peaks can be treated as additional members of the same decay scheme or as arising from complementary nuclei if they seem probable given the known partner isotope and the total neutron emission probabilities. It is apparent that cross-referencing between various sorted spectra can be extremely important in coordinating the data.

The very strong cascades through the even-even fission products<sup>1,2)</sup> of  $^{252}\text{Cf}$  proved to be very useful in this respect. In several sorted spectra, two or more of the  $2^+ \rightarrow 0^+$ ,  $4^+ \rightarrow 2^+$ , and  $6^+ \rightarrow 4^+$  transitions from different even-even isotopes of the same element were apparent, serving as an indication that the gate  $\gamma$ -ray belonged to a nucleus which seemed a probable complement to each of the even-even nuclei. In addition, if the gate gamma ray had not been previously observed to be part of the cascades through complementary even-even products, confidence in the accuracy of the even-even level schemes, supported by the data in this experiment, pointed toward an even Z odd A nucleus as the likely source. Beyond  $\gamma$ -rays matched with previous data, new lines received the same kind of attention given those in an experiment involving a single nucleus, i.e. whether sums added up to known lines, whether gates on two  $\gamma$ -rays in each case revealed the other, and the like. The possibility exists, of course, that the gate  $\gamma$  and its coincidences are from nuclei not included in previous work. This is the immediate suspicion for low energy lines not seen in the X-ray -  $\gamma$ -ray (X- $\gamma$ ) data. The errors in the energies were estimated to be  $\pm 0.2$  keV for the 0.14 cc detector and  $\pm 0.5$  keV for the 40 cc detector.

#### A. Unidentified Coincidences

For several reasons the spectra generated by many of the gates did not give conclusive evidence as to placement of the transitions recorded. Low energy  $\gamma$ -rays from elements not previously investigated

by the X-γ work or other sources could still be prominent in the total coincidence spectrum and so give rise to coincidences of unknown origin. In particular the X-ray groups of neodymium, promethium, samarium, and europium were fairly intense in the X-γ work, indicating a large number of low energy transitions of reasonably high intensity. Any coincidences arising from these elements would be difficult to pinpoint. In addition there are a few transitions which were seen strongly in more than one X-ray gate and for which the recorded coincidences were of sufficient mystery to preclude their identification. These can at least be attributed with some confidence to groups of isotopes. Table II contains the data which fit one of the above descriptions.

An example of the difficulty encountered is demonstrated by gates on two slightly overlapping peaks, one at 68.7 keV and another at 69.2 keV. The first one reveals two very strong coincidences. The 91.4 keV coincidence is supported by a gate on a 91.1 keV γ-ray which sees a 69.0 keV γ-ray intensely. The 36.5 keV designation is only approximate, as that is just above the threshold of the timing discriminator and the peak is probably distorted. The X-γ work recorded a 68.9 keV transition as by far the strongest in the total coincidence spectrum. Assigned to  $^{108}\text{Tc}$ , it was far more intense in the Tc gate than in the Cs gate. These two circumstances would seem to require that it be in cascade in  $^{108}\text{Tc}$  with a highly internal converting transition. The 36.5 keV line, broadened considerably more than by normal resolution, is probably the tail of a transition

a little below that energy. A 91.4 keV  $\gamma$ -ray was seen in the Tc and Cs gates and attributed to  $^{142}\text{Cs}$ , but it was not detected in the  $\beta$ -decay work on the same nucleus.<sup>5,9)</sup> A 138.3 keV  $\gamma$ -ray was also seen in the Tc and Cs gates but again was placed in a cesium isotope,  $^{138}\text{Cs}$ . The 138 in the 68.7 keV gate could be due to the overlap with the 69.2 keV gate, which saw a 137.5 keV  $\gamma$ -ray as easily the most profuse coincidence. A 104 keV line is seen in both of the gates as well. The solution of these problems can only be guessed at.

The gate on a 102.7 keV  $\gamma$ -ray, one of the more intense lines in the total coincidence spectrum, provided some strong coincidences but proved ambiguous on the details. Very strong lines of this energy were seen in the Mo and Ba X-ray gates as well as the Ru gate. The first was assigned to  $^{141}\text{Ba}$ , while the second was unidentified. A 138.3 keV  $\gamma$ -ray placed in  $^{141}\text{Ba}$  by that same data coupled with the coincidence with the 138.7 keV line in the present data is tempting evidence for a cascade in  $^{141}\text{Ba}$ . However three strong transitions, 181.0 keV, 199.1 keV, and 330.9 keV, are almost certainly those of the same energy in the  $^{144}\text{Ba}$  and  $^{146}\text{Ba}$  decay schemes. They imply that the 103 is in a complementary nucleus, quite possibly  $^{103}\text{Mo}$ . Confusing the issue still further is the contribution from the Ru or Xe isotope. A 457.7 keV line in the present gate suggests the  $4^+ \rightarrow 2^+$  transition in  $^{140}\text{Xe}$ , but the  $2^+ \rightarrow 0^+$   $\gamma$ -ray is not present. A possible explanation is placement of the 103 in the  $^{140}\text{Xe}$  decay scheme, but that is dubious. The 250.8 keV line is probably the one previously attributed to  $^{146}\text{Ba}$ , a conclusion which now appears erroneous. The locations of the 103 and

the  $\gamma$ -rays in coincidence with it can be limited only to one of the four elements, Mo, Ba, Ru, or Xe.

## B. [Two Step] Cascades (Table 111)

### 1. 48.5 keV Gate (Fig. 6a)

A 48.6  $\gamma$ -ray was seen very strongly in a palladium gate from the X- $\gamma$  work, the rest of the lines of about that energy being considerably weaker. The present spectrum includes a very weak line at 1276.4 keV, which is approximately the energy of a  $2^+ \rightarrow 0^+$ , reported in  $^{134}\text{Te}$ .<sup>2)</sup> The 115 keV  $6^+ \rightarrow 4^+$  and 297 keV  $4^+ \rightarrow 2^+$  transitions, completing the ground state band and mentioned elsewhere in this paper, are not seen at all, precluding the location of the 48.6  $\gamma$ -ray in a complementary nucleus to  $^{134}\text{Te}$ . The line is possibly in  $^{134}\text{Te}$  and obviously not in cascade with the 115 and 297. The fact that it is seen so strongly in the X- $\gamma$  results could mean it is the result of  $\beta$ -decay to some level within the fairly-well established ground state band.

### 2. 49.9 keV gate (Fig. 6b)

A 49.8 line seen in an I gate was attributed to  $^{116}\text{Rh}$ . An exceptionally intense 228.5  $\gamma$ -ray also seen in an I gate was assigned to  $^{132}\text{I}$ . The present data raises certain questions about the first placement. The strength of the coincidence implies they are in cascade. They are apparently the two lines observed previously in  $^{132}\text{I}$  by Fransson and Bemis.<sup>4)</sup>

The strong 55.4 and 78.4 keV lines mostly probably arose from the fact that the 49.9 transition is unresolved from a 50.3 keV  $\gamma$ -ray which appears strong in a Tc gate. In that same spectrum was an unidentified 55.1 keV line and a 78.6  $\gamma$ -ray which also appeared in the Cs gate and was placed in a Cs isotope. From the present data, a gate on a 54.9  $\gamma$ -ray, in Fig. 6c, sees quite clearly a 50.5 line but only moderately something at about 79 keV. The 50.3 keV and 55.4 keV  $\gamma$ -rays quite possibly are from a Tc isotope populated at least part of the time directly by fission.

### 3. 52.3 keV gate (Fig. 6d)

The most noticeable coincidence in this case was a still weak 264.3 line. Previous work by Hoffmann, Lawrence, and Daniels<sup>6)</sup> on  $\gamma$ -rays from  $^{146}\text{Pr}$  following  $\beta$ -decay of  $^{146}\text{Ce}$  included 52.0 keV and 264.7 keV  $\gamma$ -rays in succession.  $^{146}\text{Ce}$  is strongly populated in the fission of  $^{252}\text{Cf}$  ( $\sim 1\%$ )<sup>4)</sup> and a gate on Pr X-rays previously revealed lines of about the same energies.

### 4. 53.9 keV gate (Fig. 6e)

This  $\gamma$ -ray is in very strong coincidence with a 189.2 keV transition. An intense 54.1 keV  $\gamma$ -ray appeared in the Tc X-ray gate. Also  $\beta$ -decay work<sup>7)</sup> placed a 189.5 keV  $\gamma$ -ray in  $^{106}\text{Tc}$ . The fact that both lines are seen only in the Tc gate implies  $\beta$ -decay as the primary means of population, a good deal of which to  $^{106}\text{Tc}$  would occur due to a 3.37% fission direct intensity<sup>1)</sup> for  $^{106}\text{Mo}$ . A coincidence in  $^{106}\text{Tc}$

is the conclusion, although the assignment of the 189.5 keV transition was tentative.

5. 60.5 keV gate (Fig. 6f)

The 60.5 keV gate both in close and extended geometry, Fig. 7a, sees very strongly a 159.2 keV  $\gamma$ -ray. A 60.5 keV  $\gamma$ -ray was placed in  $^{112}\text{Rh}$  previously. A line about 159.7 keV was seen in both the Rh and I gates and left unidentified. The two sum to 219.7, whereas a 219.9 keV  $\gamma$ -ray was also seen in the Rh gate. A direct cascade in  $^{112}\text{Rh}$  is implied. The 183.1 keV line is also seen in both gates and so presumed to be somewhere in the decay scheme of  $^{112}\text{Rh}$  as well.

6. 64.3 keV gate (Fig. 6g)

This gate and two others, one for 85.5 keV and another for 129.3 keV seen in Figs. 6h and 6i, yielded three  $\gamma$ -rays in definite coincidence, each of which saw the other two. An 85.6 keV transition was previously assigned to  $^{105}\text{Tc}$  by comparison with a mass value of  $105_{-0}^{+1}$  for a similar energy from John et al.<sup>13)</sup> A 64.4 keV line was seen in the Tc and Cs gates but was left unidentified. The 129.3 keV  $\gamma$ -ray was previously unrecorded. A very tentative placement therefore is a three-stage cascade in  $^{105}\text{Tc}$ . It is entirely possible that these  $\gamma$ -rays and the 54 keV - 189 keV coincidence are in the same nucleus, either  $^{105}\text{Tc}$  or  $^{106}\text{Tc}$ , with the latter being a slightly better choice. The 53.9 keV gate saw an 86.1 keV  $\gamma$ -ray but the return coincidence

was unsubstantiated.

7. 71.6 keV gate (Fig. 6j)

The 71.6 - 138.7 coincidence indicates a cascade in a Cs isotope, as both were seen strongly in the Tc and Cs gates from X-ray -  $\gamma$ -ray. Their being in cascade is supported by the same gate in the extended geometry case, seen in Fig. 7b. The former was at that time assigned to  $^{138}\text{Cs}$  and the latter to  $^{141}\text{Cs}$ . The basis of those assignments was some mass-separated data of Alvager *et al.*<sup>5)</sup> and the energy agreement was much better in the  $^{138}\text{Cs}$  case. On that basis, this cascade seems to be in  $^{138}\text{Cs}$ .

8. 76.7 keV gate (Fig. 6k)

A 76.5  $\gamma$ -ray was present in both the Tc and Cs gates and was given to  $^{141}\text{Cs}$ . A 160.7 keV  $\gamma$ -ray was seen in the Tc gate and was possibly obscured in the Cs gate due to a strong peak of another energy nearby. The very strong coincidence with a 160.5 keV line, also evident in the EG data of Fig. 7c, indicates a cascade in  $^{141}\text{Cs}$ . The coincidence with the 268.9  $\gamma$ -ray is less certain. The Xe gate saw a 76.6 keV line and also a 270 keV line from  $^{106}\text{Ru}$ , so a possible source is  $^{106}\text{Ru}$ .

9. 86.3 keV gate (Fig. 6l)

This gate contained two  $\gamma$ -rays, 90.5 and 154.3, which were seen in the X- $\gamma$  data in the Tc gate (90.3 keV) and Tc and Cs gates

(154.1 keV), respectively. In addition, an 86.2 keV  $\gamma$ -ray was seen moderately well in the Cs gate. The 90.3  $\gamma$ -ray was assigned to  $^{142}\text{Cs}$  in that work.  $\beta$ -decay work by Larsen, Talbert, and McConnell<sup>9)</sup> did not reveal such a line in  $^{142}\text{Cs}$ . The 154.3  $\gamma$ -ray was assigned to  $^{138}\text{Cs}$  on the basis of  $\beta$ -decay work of Alvager et al.<sup>5)</sup> Close examination of the X- $\gamma$  spectra shows that 86.2 and 90.3 lines could possibly be obscured by strong neighboring peaks in the Tc and Cs gates, respectively. All of the data point toward the two  $\gamma$ -rays as being in cascade with the gate gamma in the  $^{138}\text{Cs}$  nucleus.

#### 10. 115.5 keV gate (Fig. 6m)

This spectrum consists principally of the  $4^+ \rightarrow 2^+$  297 keV transition and  $2^+ \rightarrow 0^+$  1276 transition reported as following a 115 keV  $6^+ \rightarrow 4^+$  transition in  $^{134}\text{Te}$ .<sup>2)</sup>

#### 11. 123.2 keV gate (Fig. 6n)

A strong coincidence in this spectrum with a 125.8 keV  $\gamma$ -ray and a gate on a 125.3 line, in Fig. 6p showing coincidence with a 123.5 keV  $\gamma$ -ray, are strong evidence for a cascade. The best candidate available is  $^{109}\text{Tc}$ . A 123.1 keV line was seen in both Tc and Cs gates and attributed to  $^{109}\text{Tc}$  by the X- $\gamma$  work.  $\beta$ -decay work<sup>7)</sup> assigned a 125.5 keV transition to  $^{108}\text{Tc}$  but with a low confidence rating.

## 12. 126.4 keV gate (Fig. 6g)

This gate plus a gate on a 159.3 keV  $\gamma$ -ray shown in Fig. 6r reveal a strong coincidence between those two lines. The EG data from a gate on the lower of the two energies suggests a cascade, as seen in Fig. 7d. Both of these energies were seen in the Nb and La gates with a 158.9 assigned to  $^{147}\text{La}$ . On that basis the cascade is tentatively placed in  $^{147}\text{La}$ .

### C. Rudimentary Energy Level Schemes

#### 1. $^{105}\text{Mo}$

Coincidence information from several different lines tied together nicely and pointed toward decays in this odd A isotope of molybdenum. Gates on  $\gamma$ -rays of energies 94.9 keV, 138.1 keV, and 144.9 keV yielded the spectra in Figs. 8a-c and Table IV. Each of the three  $\gamma$ -rays sees the other two strongly, as well as having appeared in both the Mo and Ba gates of the previous X- $\gamma$  data. From that work the 94.9 keV line was assigned to  $^{106}\text{Mo}$  based on correlation with the paper of Watson et al.<sup>14)</sup> The 138.1 keV  $\gamma$ -ray was attributed to  $^{141}\text{Ba}$ , which means there may be two lines at about that energy. A 144.7 keV transition was placed in  $^{104}\text{Mo}$  but that assignment was based on the data of John et al.<sup>13)</sup> which reported a  $104_{-0}^{+1}$  value for the mass, indicating it could be from mass 105. The only EG data with sufficient statistics to show anything convincing was the gate on the 94.9 keV  $\gamma$ -ray, Fig. 9a.

The fact that several strong lines from the two even-even

isotopes  $^{142}\text{Ba}$  and  $^{144}\text{Ba}$  are present in the 94.9 gate also indicates a complementary Mo nucleus. A total neutron emission of 3 in the first case and 5 in the second, both feasible values, would allow the two to be complements of  $^{105}\text{Mo}$ . Information received from Wilhelmy et al.<sup>15)</sup> for  $^{105}\text{Mo}$  was almost identical to the data presented here. The weight of evidence is great for a three-stage cascade in  $^{105}\text{Mo}$  as shown in Fig. 10. The order of the transitions is not a certain thing but the strength of the 95-138 coincidence is some indication that they are below the 145 keV transition. Other lines seen in the 94.9 gate which Wilhelmy et al.<sup>15)</sup> also saw for  $^{105}\text{Mo}$  are one at 246.5 keV and another at 417.7 keV. The 246 was seen weakly here and not at all in the other gates. The 418 was seen moderately strong, as well as being very weak in the other two gates. Their placement as shown in Fig. 10 is extremely tentative.

Some additional information is to be found in the 94.9 keV gate. A strong coincidence with a 117.6 keV  $\gamma$ -ray which was not seen in the other gates and which escaped detection by Wilhelmy indicates a transition in an odd Ba isotope complementary to  $^{105}\text{Mo}$ . However, the EC data also reveals a  $\gamma$ -ray of about the same energy, implying it is in the same scheme. A 117.3 keV transition seen in the X- $\gamma$  work in the Mo - Ba gates was assigned with doubt to  $^{142}\text{Ba}$ , a nucleus which received attention in a post  $\beta$ -decay investigation by Larsen et al.<sup>9)</sup> The latter group detected no such  $\gamma$ -ray. John et al.<sup>13)</sup> did and gave it mass  $144 \pm 1$ . Two possibilities seem to be  $^{143}\text{Ba}$  and  $^{145}\text{Ba}$ . A gate on a 117.6 keV  $\gamma$ -ray resulted in the spectrum seen in Fig. 8d and the

values in Table IV. Most obvious are strong coincidences with  $\gamma$ -rays of 283.0 keV and 342.8 keV, both seen strongly as well in the 94.9 keV gate and probably cascade members with the 117. The clue to their location is found in the presence of  $\gamma$ -rays apparently from the even-even isotopes  $^{102}\text{Mo}$ ,  $^{104}\text{Mo}$  and  $^{106}\text{Mo}$ . Feasible complements to these two in the binary fission of  $^{252}\text{Cf}$  are  $^{143}\text{Ba}$  and  $^{145}\text{Ba}$ , supporting the mass data of John et al.<sup>13)</sup> Since  $^{145}\text{Ba}$  would require that only a single neutron be boiled off, for it to be a post-neutron complement of  $^{106}\text{Mo}$ ,  $^{143}\text{Ba}$  is the logical choice as the nucleus emitting the 117.6 keV line, as well as cascades above that one involving the 283.0 keV and 342.8 keV  $\gamma$ -rays. It is possible that another  $\gamma$ -ray of about that energy is involved in the decay of  $^{105}\text{Mo}$ .

There is also some evidence that a  $\gamma$ -ray of about 282.6 keV is involved in the level scheme of  $^{105}\text{Mo}$ . The fact that that particular line is much stronger in comparison to the 342.8 line in the 94.9 keV gate than in the 117.6 keV gate indicates that the peak is at least partially derived from a coincidence in  $^{105}\text{Mo}$ . Wilhelm also saw a 283. Supporting this conclusion is the fact that it fits well in the decay scheme, just about equalling the sum of the 138.1 keV and 144.7 keV transitions.

## 2. $^{109}\text{Ru}$

Figs. 11a and 11b present spectra derived from gates on 74.2 keV and 98.3 keV  $\gamma$ -rays in the low-energy total coincidence spectrum. Table V has the tabulations. The X- $\gamma$  work had assigned a 98.5 keV

transition to  $^{108}\text{Ru}$  with a good bit of doubt and a 131.8 keV transition to  $^{110}\text{Ru}$ , an even-even isotope. The validity of the reported even-even level scheme,<sup>1)</sup> supported by the present data, precludes  $^{110}\text{Ru}$  as a choice. The 482.2 keV and 587.8 keV  $\gamma$ -rays are apparently the  $4^+ \rightarrow 2^+$  and  $2^+ \rightarrow 0^+$  transitions in  $^{138}\text{Xe}$  previously reported<sup>2)</sup> and indicate either  $^{111}\text{Ru}$  or  $^{109}\text{Ru}$ . Other data in this paper for  $^{111}\text{Ru}$  does not include these lines. In addition, the experiment performed by Wilhelmy et al.<sup>15)</sup> assigned 74 keV, 98 keV, 172 keV, 193 keV and 374 keV transitions to  $^{109}\text{Ru}$  but was unable to provide any placements due to lack of coincidence data. The present data is extremely convincing that at least the partial decay scheme of  $^{109}\text{Ru}$  looks like Fig. 12.

The fact that the 374 is weaker in the 98 keV gate than the 74 keV gate indicates the 74 is above the 98 in order. The latter two definitely seem to be in succession, as attested to the 172 seen by Wilhelmy and a 172 seen in both the Ru and Xe X-ray gates. In addition, Wilhelmy recorded a greater  $\lambda$ /fission for the 98. One problem is the overlap of the second gate with another strong 98.1 line found in the Zr - Ce gates and questionably identified. The strong 133.8 keV transition in the present  $\gamma$ -ray gate was also seen in the two X-ray gates and attributed to  $^{148}\text{Ce}$  on the basis of a  $148_{-0}^{+1}$  mass assignment by John et al.,<sup>13)</sup> but the energy agreement was poor. Recently reported is a 98.3 keV transition in  $^{101}\text{Zr}$ <sup>16)</sup> and that is the probable location of the 98 - 134 cascade. So the 98.3 keV gate is a combined spectrum and the 374 might be expected to be down relative to background for that reason also. The intensity of the 133.8 keV  $\gamma$ -ray unfortunately

prevents knowledge of whether the 98 is in coincidence with the 131.8 keV  $\gamma$ -ray as the 74 is. The placement in  $^{106}\text{Ru}$  can thus not be supported or refuted on that basis.

### 3. $^{111}\text{Ru}$

Data from gates on  $\gamma$ -rays of 62.8 keV, 75.9 keV, 103.9 keV, and 150.5 keV energy are presented in Figs. 13a, 13d and Table VI. The EG data for 62.9 keV and 104.1 keV gates, the strongest of the group in the total coincidence spectrum, are shown in Figs. 9a and 9b. The low-energy coincidence information is clearcut. The 63 sees a 76, 104, and 150. The 104 sees the 63, 76, and 150, except in the EG case where a pyrex disk between source and detector attenuated the lower energy keV  $\gamma$ -rays. In that particular spectrum lines are indicated but not conclusively. The 150 sees the 63, 76, and the 104. Finally the 76 sees the 63, 104, 150 and a 166.9 keV  $\gamma$ -ray which is just about the sum of the 63 and 104. Referring once again to the previous X-ray gates, a 104.0 keV line and a 150.5 keV line were seen and placed in  $^{111}\text{Ru}$ , with a 63.0  $\gamma$ -ray unidentified. Data from Wilhelm *et al.*<sup>15)</sup> again supports the present work for transitions in  $^{111}\text{Ru}$ . They were unable to obtain coincidence data on the 63 keV line but found a smaller  $Z$ /fission yield than for the 104. The level scheme shown in Fig. 14 nicely accounts for the present and previous data.

The 722.8 keV line seen extremely strongly in the 63 gate is a problem. Since it is not seen at all by the other gates, it cannot be from a complementary nucleus and therefore it must bypass them.

This is impossible in the case of the 104 if it is actually below the 63 keV transition. A 357.3 keV  $\gamma$ -ray is seen at least weakly in each of the four gates. Being the strongest in the 76 gate, presumably it is a cascade directly to the 384 level.

#### 4. $^{146}\text{La}$

Figs. 15a and 15b contain spectra from gates on 81.9 keV and 130.6 keV  $\gamma$ -rays. As shown in Table VII, the lower energy line has been seen previously and attributed to  $^{146}\text{La}$ , as have the 104.1 keV and 363.6 keV transitions<sup>11,12)</sup> seen in the first gate. A 130.6 keV  $\gamma$ -ray was also placed in  $^{146}\text{La}$  by the same work. The partial energy scheme in Fig. 16 is indicated by this data. A line of 269.9 keV was seen in the present gate and previous X- $\gamma$  data, while a 212.7 keV  $\gamma$ -ray was recorded in the La gate from the latter. These values lend credence to the diagram.

#### IV. Discussion

The level schemes shown in Figs. 10, 12, 14, and 16 should only be regarded as relative partial schemes. The energies given are taken where possible from the X- $\gamma$  work, since those separated spectra should be more accurate. The "0" level is more of a reference point than an indication of the ground state, although the intensity of these lines would indicate that they lie at least in the lower part of the complete schemes. In several cases the order of the transitions is

obscure. The 98 keV  $\gamma$ -ray was placed below the 74 keV line in  $^{109}\text{Ru}$  strictly on the basis of a greater  $\lambda/\text{fission}$  for the former reported by Wilhelmy.<sup>15)</sup> This placement is supported by the difference in the intensity of the 374 keV  $\gamma$ -ray in the two gates. The 63 keV and 104 keV transitions in  $^{111}\text{Ru}$  are placed again on the basis of the  $\lambda/\text{fission}$  values from Wilhelmy.<sup>15)</sup> These two could be switched however, as might be indicated by the strong coincidence between a 722.8 keV  $\gamma$ -ray and the first but not the second. Assuming they are both below the 723, the one below the other should see anything the latter sees. An alternative solution is that the 63 - 723 coincidence involves another 63 keV transition from an unidentified source. It must be kept in mind that these schemes are only suggestions which explain the data.

A natural complement to these data would be  $\beta$ -decay studies on each of the four nuclei. The affirmation of the order of certain transitions and the spin-parity information resulting from the selectivity of the  $\beta$ -decay process would greatly clarify the work presented here. In fact, once more of the schemes were made known, these data would take on new significance in that they represent at least to some extent the population of various states which would escape a  $\beta$ -decay study. As has been noted before,<sup>17)</sup> the effect of the fission process and subsequent neutron boiloff can be conveniently thought of as an  $(\alpha, 2n)$  reaction which is capable of populating high spin as well as lower spin states. The subsequent decays should involve in some cases states which escape population by  $\beta$ -decay.

An additional experiment which would supply information on

spins and parities is a  $\gamma$ -ray - internal conversion electron coincidence system. The K/L ratios could be used to infer the multipolarities and thereby the spins.

Gates on  $\gamma$ -rays of energies 192.3 keV, 171.9 keV, 198.6 keV, and 158.9 keV, corresponding to the energies of the  $2^+ \rightarrow 0^+$  transition in four of the most heavily populated even-even nuclei,  $^{104}\text{Mo}$ ,  $^{106}\text{Mo}$ ,  $^{144}\text{Ba}$ , and  $^{148}\text{Ce}$ , respectively, failed to reveal coincidences with any of the low energy lines assigned to them by the X- $\gamma$  experiments. The gated spectra consisted primarily of the values for the various transitions in the ground state bands previously reported.<sup>1,2)</sup> In fact two of these lines, 94.9 keV and 144.7 keV, were incorporated in the  $^{105}\text{Mo}$  decay scheme. The majority of the  $\gamma$ -rays so placed are probably off by 1 a.m.u. due to the uncertainty in mass calculations of the previous data.

## References

\* Research supported in part by the Advanced Research Projects Agency of the Department of Defense and monitored by the Office of Naval Research under Contract No. N00014-67-A-0126-0012.

† Present address: Department of Physics, Kansas State University, Manhattan, Kansas 66502.

1. E. Cheifetz, R. C. Jared, S. G. Thompson, and J. B. Wilhelmy, *Phys. Rev. Letters* 25, 38 (1970).
2. J. B. Wilhelmy, S. G. Thompson, R. C. Jared, and E. Cheifetz, *Phys. Rev. Letters* 25, 1122 (1970).
3. J. W. Gruter, K. Sistemich, P. Ambruster, J. Eidens, and H. Lavin, *Phys. Letters* 33B, 474 (1970).
4. K. Fransson and C. E. Bemis, Jr., *Nucl. Phys.* 78, 207 (1965).
5. T. Alvager, R. A. Neumann, R. F. Petry, G. Sidenius, and T. Derrah Thomas, *Phys. Rev.* 167, 1105 (1968).
6. D. C. Hoffman, F. O. Lawrence, and W. R. Daniels, *Phys. Rev.* 172, 1239 (1968).
7. J. B. Wilhelmy, University of California Radiation Laboratory No. UCRL-18978, 1969 (unpublished).
8. W. C. Shick, Jr., W. L. Talbert, Jr., and J. R. McConnell, *Phys. Rev. C* 4, 507 (1971).

9. J. T. Larsen, W. L. Talbert, Jr., and J. R. McConnell, Phys. Rev. C3, 1372 (1971).
10. S. Borg et al., Annual Report, Research Institute for Physics, Stockholm, Sweden, 1970 (unpublished).
11. F. F. Hopkins, G. W. Phillips, J. R. White, C. Fred Moore, and Patrick Richard, Phys. Rev. C4, 1927 (1971).
12. F. F. Hopkins, J. R. White, G. W. Phillips, C. Fred Moore, and Patrick Richard, Phys. Rev. C5, 1015 (1972).
13. W. John, F. W. Guy, and J. J. Wesolowski, Phys. Rev. C2, 1451 (1970).
14. R. L. Watson, J. B. Wilhelmy, R. C. Jared, C. Ruge, H. R. Bowman, S. G. Thompson, and J. O. Rasmussen, Nucl. Phys. A141, 449 (1970).
15. J. B. Wilhelmy et al., private communication.
16. J. B. Wilhelmy, E. Cheifetz, R. C. Jared, S. G. Thompson, and H. R. Bowman, Phys. Rev. C5, 2041 (1972).
17. E. Cheifetz, J. B. Wilhelmy, R. C. Jared, and S. G. Thompson, Phys. Rev. C6, 1913 (1971).

TABLE I: Energies of  $\gamma$ -rays Gated on (keV)

48.5	70.3	94.9	129.3
49.9	71.6	97.0	130.6
50.7	72.6	98.3	136.0
52.3	74.2	(101.0)	[138.1]
53.3	75.9	102.7	[138.5]
53.9	76.7	103.9	141.0
54.9	77.7	106.2	[144.9]
56.1	78.8	(108.3)	150.5
58.1	80.0	(109.9)	152.0
59.7	[81.9]	112.7	[158.9]
60.5	[82.5]	115.5	(159.3)
61.8	84.3	117.6	(162.4)
62.8	85.5	119.6	171.9
64.3	86.3	122.0	192.3
[65.8]	87.4	123.2	199.6
57.1	89.2	125.3	
[68.7]	(91.1)	[126.4]	
[69.2]	[91.8]	128.0	

- [ ] - Large width indicating unresolved lines.  
 ( ) - Very low intensity, so energy uncertain.

TABLE II: Coincidences Involving Unidentified  $\gamma$ -rays

Gate $\gamma$ -ray (keV) (Possible Origin)	Coincidences (keV)
58.1 Y, Pr, Nb, La, Tc, or Cs	90.3, 102.8, 125.5, 154.3, 159.1, 219.2
65.8 Nb, La, Rh or I	(59.8), <u>71.9</u> , 118.4, 126.5, <u>138.4</u> , (142.4), <u>159.4</u> , <u>172.1</u> , (182.9), (186.5), (218.4), (240.9), (268.1), (313.8), (358.4)
68.7 Tc, Cs, or Pr	<u>36.5</u> , (46.5), (69.6), (86.5), <u>91.4</u> , <u>104</u> , 118.1, <u>138.0</u> , 190.6, (212.2), (241.5), <u>375.2</u> , (420.7)
69.2 <sup>108</sup> Tc or Pr	<u>103.8</u> , <u>118.2</u> , <u>137.5</u> , 289.3, (297.9), (369.2), (387.7), (436.8)
70.3 Zr or Ce	106.1, 154.3, 163.3, <u>192.4</u> , (929.9), (1359.3)
72.6	134.6, <u>164.1</u> , (172.9), (247.1)
78.8 Tc or Cs	80.5, (103.8), (112.2), 138.1, (250.1), <u>303.2</u>
82.5 Zr, Ce, Xe, or Ru	(76.1), 100.3, 109.4, 117.8, 127.5, <u>143.4</u> , 153.6, 159.2, 244.6, (250.7), 283.2, (638.8)
87.4 <sup>136</sup> I	(104.5), <u>135.6</u> , 166.1, <u>203.8</u> , 211.7
89.2 Tc or Cs	104.2, <u>148.0</u>

TABLE II: Cont'd

91.1 Tc, Cs, Nb or La	<u>69.0</u> , <u>93.5</u> , 150.4, 158.4, (163.4), <u>314.2</u> , <u>375.4</u>
91.8 Tc, Cs, Rh, n I	<u>91.5</u> , 118.5, 150.5, 158.4, <u>164.5</u> , <u>314.8</u>
101.0 Y or Pr	<u>250.4</u> , (289.0), (696.1), (722.7)
102.7 Mo, Ru, or Xe	109.0, 112.9, 125.2, <u>138.7</u> , 144.5, (159.2), (164.8), 181.0, 199.1, <u>250.8</u> , 330.9, (362.6), 457.7, 537.8, <u>594.1</u>
108.3 Tc, Cs, Xe, or Ru	<u>103.3</u> , <u>138.9</u> , 142.2, (357.6)
119.6 <sup>109</sup> Tc, Nb, or La	<u>136.1</u> , (167.2), 211.5, (276.3), (443.6)
122.0 Y, Zr, or Ce	<u>130.1</u> , 535.1
136.0 Zr, Ce, Nb, or La	(69.7), <u>119.5</u> , <u>210.4</u> , (249.3), (276.0)
138.5 Mo, Ba, Tc, Cs, Ru, or Xe	71.9, 95.4, <u>103.1</u> , 108.3, (145.1), (199.2)

\_\_\_\_\_ - Indicates strong coincidence

( ) - Indicates weak coincidence

TABLE III: Coincidences Involved in Identified Cascades

Gate $\gamma$ -ray (keV)	Coincidences (keV)
48.5 [ $^{234}\text{Tc}$ ]	58.4, 91.9, 96.1, 172.0, 192.5, 394.2, (587.4), (1276.4)*
49.9 [ $^{132}\text{I}$ ]	(43.0), <u>55.4</u> , <u>78.4</u> , (117.3), (192.1), (211.7), (218.5), <u>228.2*</u> , (241.5), (249.7), (576.8), 640.2
54.9	<u>50.5</u> , (69.1), 79.3, 91.5, 103.8, 136.3, (159.1), 212.4, 241.5
52.3 [ $^{146}\text{Pr}$ ]	<u>264.3*</u>
53.9 [ $^{106}\text{Tc}$ ]	<u>82.8</u> , <u>86.1</u> , 97.1, 103.8, 135.6, <u>189.2*</u> , 249.0, (315.1), (364.2), 429.1, 594.1, 617.6
60.5 [ $^{112}\text{Rh}$ ]	98.8, 103.8, <u>159.2*</u> , <u>183.1*</u> , 241.6, 268.3, (399.6), (1131.3)
64.3 [ $^{105}\text{Tc}$ ]	<u>85.8*</u> , 97.2, 125.5, <u>129.3*</u> , 142.7, 158.4, 172.1, (313.7), 534.0
85.5 [ $^{105}\text{Tc}$ ]	<u>64.7*</u> , <u>129.3*</u> , <u>218.3*</u> , 246.7, (313.8), (340.0), (510.6), (524.1)
129.3 [ $^{105}\text{Tc}$ ]	64.7*, 85.9*, (129.8)

TABLE III: Cont'd

71.6 [ <sup>138</sup> Cs]	(66.1), <u>138.7*</u> , 159.8, 205.2, (282.3), 292.4, 357.9, 369.1, 451.7
76.7 [ <sup>141</sup> Cs]	<u>160.5*</u> , 172.9, 204.3, <u>258.9</u> , 363.6, 369.2, (396.5), (422.2), (435.4), (446.1)
86.3 [ <sup>138</sup> Cs]	<u>90.5</u> , <u>154.3*</u> , 249.0, (371.6)
115.5 [ <sup>134</sup> Te]	(69.7), (104.0), 126.3, 249.4, <u>296.6*</u> , <u>1276.2*</u>
123.2 [ <sup>109</sup> Tc]	<u>125.8*</u> , 154.3
125.3 [ <sup>109</sup> Tc]	(91.2), (97.7), (103.4), <u>123.5*</u> , 154.5, <u>158.9</u> , 198.5
126.4 [ <sup>147</sup> La]	(98.8), (104.5), <u>159.2*</u> , 232.0, 301.9
159.3 [ <sup>147</sup> La]	<u>126.5*</u> , 143.0, 183.3, 219.5, (242.2), (269.3)

\_\_\_\_\_ - Indicates strong coincidence

( ) - Indicates weak coincidence

\* - In cascade with gate  $\gamma$ -ray in isotope indicated

TABLE IV: Coincidences in  $^{105}\text{Mo}$ 

Gate $\gamma$ -ray (keV)	Coincidences (keV)	Origin
94.9	<u>113.1</u> <u>117.5</u> <u>138.2</u> <u>145.2</u> 164.8 <u>199.2</u> <u>245.7</u> 253.5 <u>282.6</u> <u>330.4</u> <u>342.8</u> <u>359.1</u> (390.0) 417.7 (430.5)	$^{105}\text{Mo}$  $^{105}\text{Mo}$ $^{105}\text{Mo}$  $^{144}\text{Ba}^a$   $^{144}\text{Ba}^a$  $^{142}\text{Ba}^a$  $^{144}\text{Ba}^a$
138.1	70.9 <u>95.3</u> 103.3 117.7 131.8 138.0 <u>145.1</u> <u>199.4</u> (269.7) (330.9) (358.3)	$^{105}\text{Mo}$  $^{105}\text{Mo}$   $^{105}\text{Mo}$ $^{144}\text{Ba}^a$  $^{144}\text{Ba}^a$
144.9	<u>95.3</u> 103.3 <u>138.2</u> <u>199.2</u> (232.4) (246.5) (250.0)	$^{105}\text{Mo}$ $^{105}\text{Mo}$  $^{105}\text{Mo}$ $^{144}\text{Ba}^a$  $^{105}\text{Mo}$

TABLE IV: Cont'd

117.6	(69.4) (82.8) 95.3 (98.4) (103.3) 124.9 138.2 152.1 171.7 192.2 212.4 (250.6) <u>283.0</u> <u>342.8</u> 350.2 (368.1) (492.3)	Ba isotope  105Mo   105Mo 102Zr <sup>b</sup> 106Mo <sup>b</sup> 104Mo <sup>b</sup> 100Zr <sup>b</sup>   106Mo <sup>b</sup> 104Mo <sup>b</sup>
-------	---	--

\_\_\_\_\_ - Indicates strong coincidence

( ) - Indicates weak coincidence

a - See Ref. 2

b - See Ref. 1

TABLE V: Coincidences in  $^{109}\text{Ru}$ 

Gate $\gamma$ -ray (keV)	Coincidences (keV)	Origin
74.2	(70.0)	$^{109}\text{Ru}$
	91.9	
	<u>98.5</u>	$^{109}\text{Ru}$
	132.2	$^{109}\text{Ru}$
	159.2	
	314.2	
	<u>374.2</u>	$^{109}\text{Ru}$
	482.2	$^{138}\text{Xe}^a$
	587.8	$^{138}\text{Xe}^a$
	98.3	74.7
118.4		$^{109}\text{Ru}$
<u>133.8</u>		
158.7		
176.7		
218.3		
222.7		
250.1		
258.4		
(282.6)		
295.1		
374.4		$^{109}\text{Ru}$
386.4		
482.2		$^{138}\text{Xe}^a$

\_\_\_\_\_ - Indicates strong coincidence

( ) - Indicates weak coincidence

a - See Ref. 2

TABLE VI: Coincidences in  $^{111}\text{Ru}$ 

Gate $\gamma$ -ray (keV)	Coincidences (keV)	Origin
62.8	<u>76.4</u> <u>104.0</u> <u>150.4</u> 284.1 357.4 (438.9) (482.5) 587.7 <u>722.8</u>	$^{111}\text{Ru}$ $^{111}\text{Ru}$ $^{111}\text{Ru}$ $^{111}\text{Ru}$  $^{111}\text{Ru}$  $^{138}\text{Xe}^a$ $^{138}\text{Xe}^a$
75.9	<u>63.4</u> <u>104.2</u> <u>150.4</u> <u>166.9</u> 174.5 302.7 (315.1) <u>357.3</u> (398.9) (482.4) (513.7) (587.8)	$^{111}\text{Ru}$ $^{111}\text{Ru}$ $^{111}\text{Ru}$ $^{111}\text{Ru}$ $^{111}\text{Ru}$  $^{111}\text{Ru}$  $^{138}\text{Xe}^a$  $^{138}\text{Xe}^a$
103.9	63.4 76.3 82.4 110.8 (115.0) (125.6) 138.8 <u>150.5</u> <u>357.3</u> 387.0 429.9 482.2	$^{111}\text{Ru}$ $^{111}\text{Ru}$ $^{111}\text{Ru}$     $^{111}\text{Ru}$ $^{111}\text{Ru}$   $^{138}\text{Xe}^a$

TABLE VI: Cont'd

103.9	513.8 569.7 587.8 <u>695.6</u> <u>972.3</u>	$^{138}\text{Xe}^a$
150.5	63.5 <u>76.3</u> 91.8 <u>104.1</u> 139.1 166.2 (357.7)	$^{111}\text{Ru}$ $^{111}\text{Ru}$ $^{111}\text{Ru}$  $^{111}\text{Ru}$  $^{111}\text{Ru}$ $^{111}\text{Ru}$

\_\_\_\_\_ - Indicates strong coincidence

( ) - Indicates weak coincidence

a - See Ref. 2



## Figure Captions

- Fig. 1 Coincidence electronics diagram.
- Fig. 2 Shielding apparatus used in extended geometry experiment.
- Fig. 3 0.14 cc total coincidence spectrum accumulated over 36 hours of run time.
- Fig. 4 40 cc total coincidence spectrum accumulated over 36 hours of run time.
- Fig. 5 0.14 cc total coincidence spectrum from extended geometry experiment.
- Fig. 6a Sorted spectrum for gate on 48.5 keV  $\gamma$ -ray.
- 6b Sorted spectrum for gate on 49.9 keV  $\gamma$ -ray.
- 6c Sorted spectrum for gate on 54.9 keV  $\gamma$ -ray.
- 6d Sorted spectrum for gate on 52.3 keV  $\gamma$ -ray.
- 6e Sorted spectrum for gate on 53.9 keV  $\gamma$ -ray.
- 6f Sorted spectrum for gate on 60.5 keV  $\gamma$ -ray.
- 6g Sorted spectrum for gate on 64.3 keV  $\gamma$ -ray.
- 6h Sorted spectrum for gate on 85.5 keV  $\gamma$ -ray.
- 6i Sorted spectrum for gate on 129.3 keV  $\gamma$ -ray.
- 6j Sorted spectrum for gate on 71.6 keV  $\gamma$ -ray.
- 6k Sorted spectrum for gate on 76.7 keV  $\gamma$ -ray.
- 6l Sorted spectrum for gate on 86.3 keV  $\gamma$ -ray.

Fig. 6m Sorted spectrum for gate on 115.5 keV  $\gamma$ -ray.

6n Sorted spectrum for gate on 123.2 keV  $\gamma$ -ray.

6p Sorted spectrum for gate on 125.3 keV  $\gamma$ -ray.

6q Sorted spectrum for gate on 126.4 keV  $\gamma$ -ray.

6r Sorted spectrum for gate on 159.3 keV  $\gamma$ -ray.

Fig. 7a Extended geometry data for 60.5 keV gate.

7b Extended geometry data for 71.6 keV gate.

7c Extended geometry data for 76.7 keV gate.

7d Extended geometry data for 126.4 keV gate.

Fig. 8a Sorted spectrum from gate on 94.9 keV  $\gamma$ -ray.

8b Sorted spectrum from gate on 138.1 keV  $\gamma$ -ray.

8c Sorted spectrum from gate on 144.9 keV  $\gamma$ -ray.

8d Sorted spectrum from gate on 117.6 keV  $\gamma$ -ray.

Fig. 9a Sorted spectrum from extended geometry case for gate on 94.9 keV  $\gamma$ -ray.

9b Sorted spectrum from extended geometry case for gate on 62.7 keV  $\gamma$ -ray.

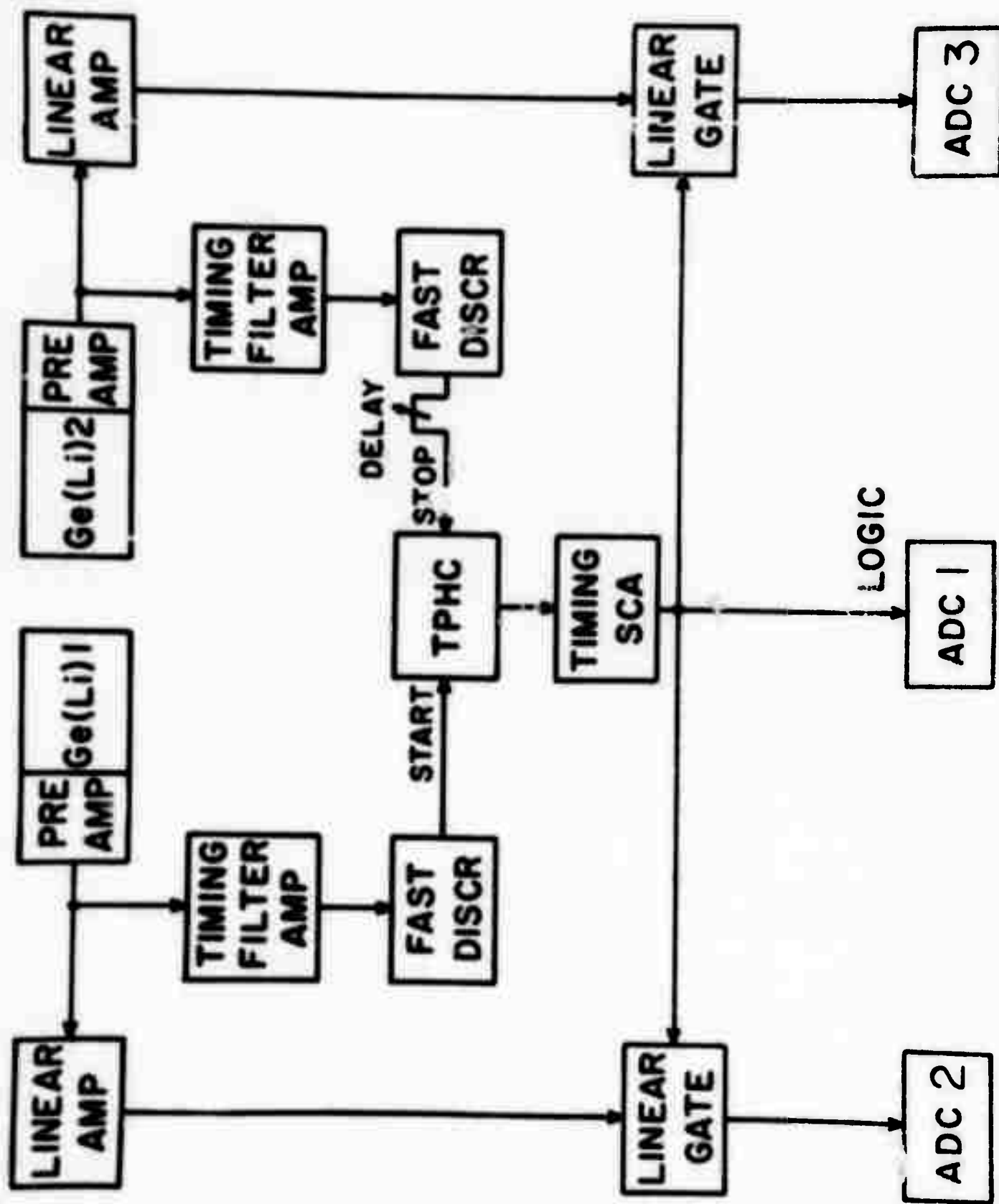
9c Sorted spectrum from extended geometry case for gate on 104.1 keV  $\gamma$ -ray.

Fig. 10 Partial decay scheme for  $^{105}\text{Mo}$ .

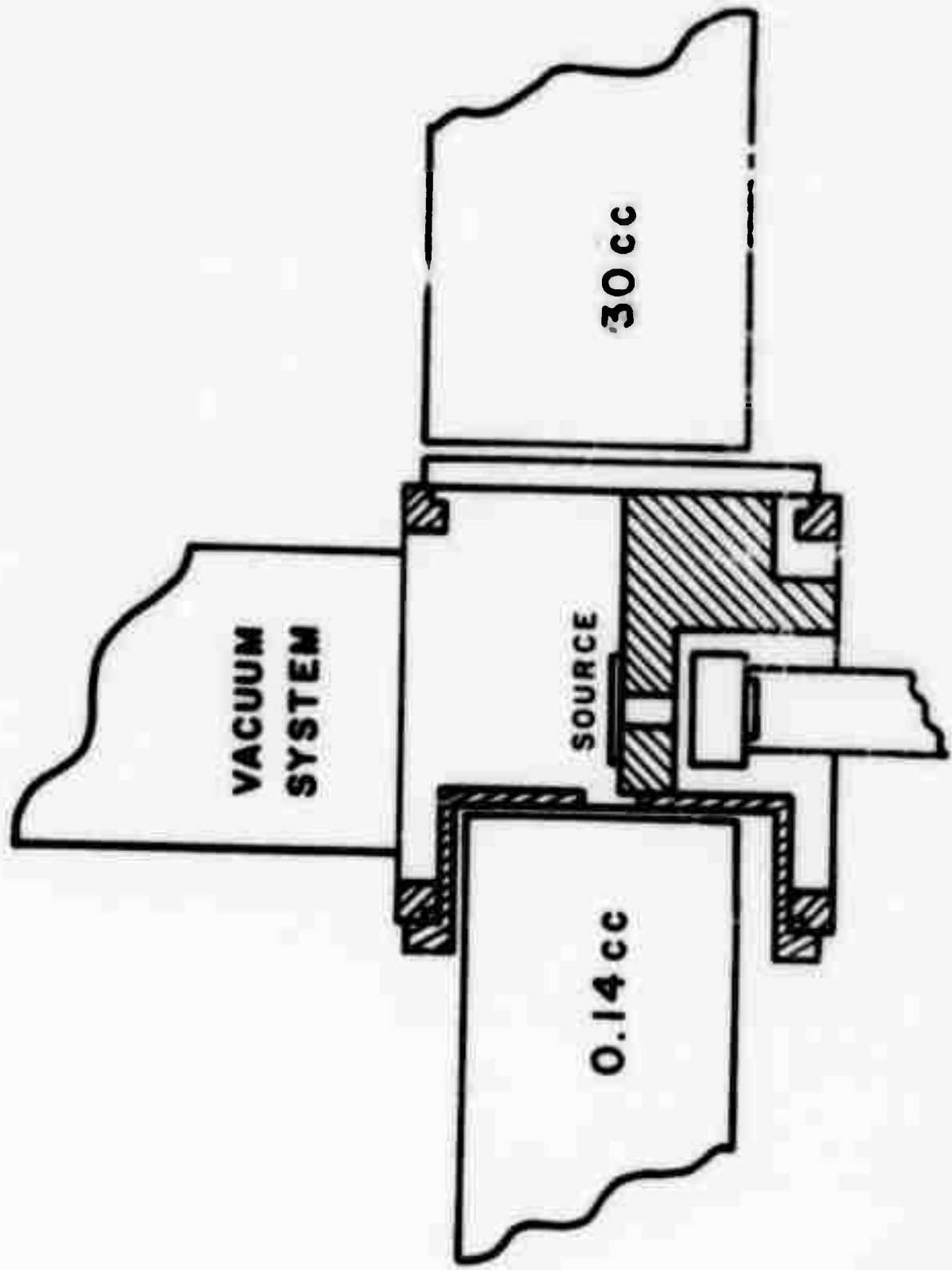
Fig. 11a Sorted spectrum from gate on 74.2 keV  $\gamma$ -ray.

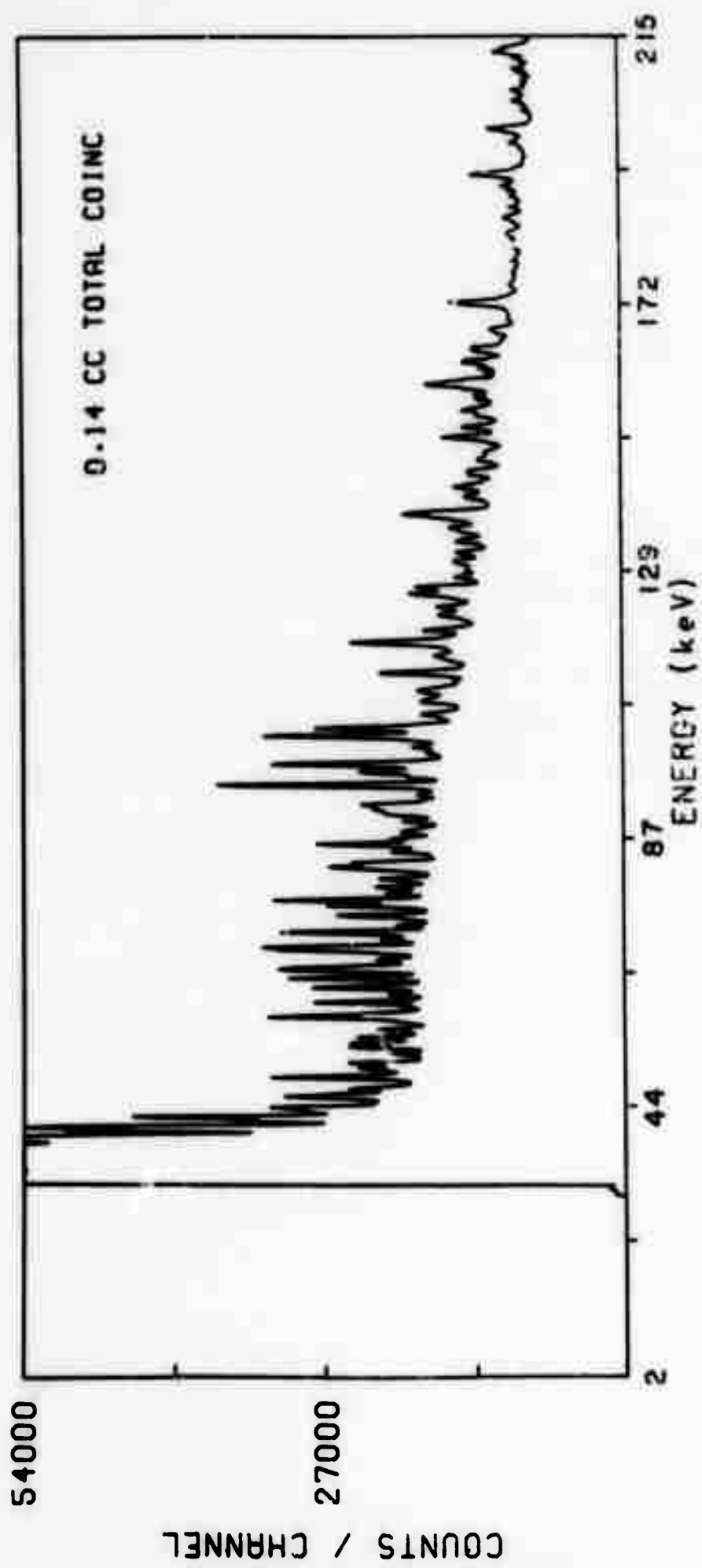
11b Sorted spectrum from gate on 98.3 keV  $\gamma$ -ray.

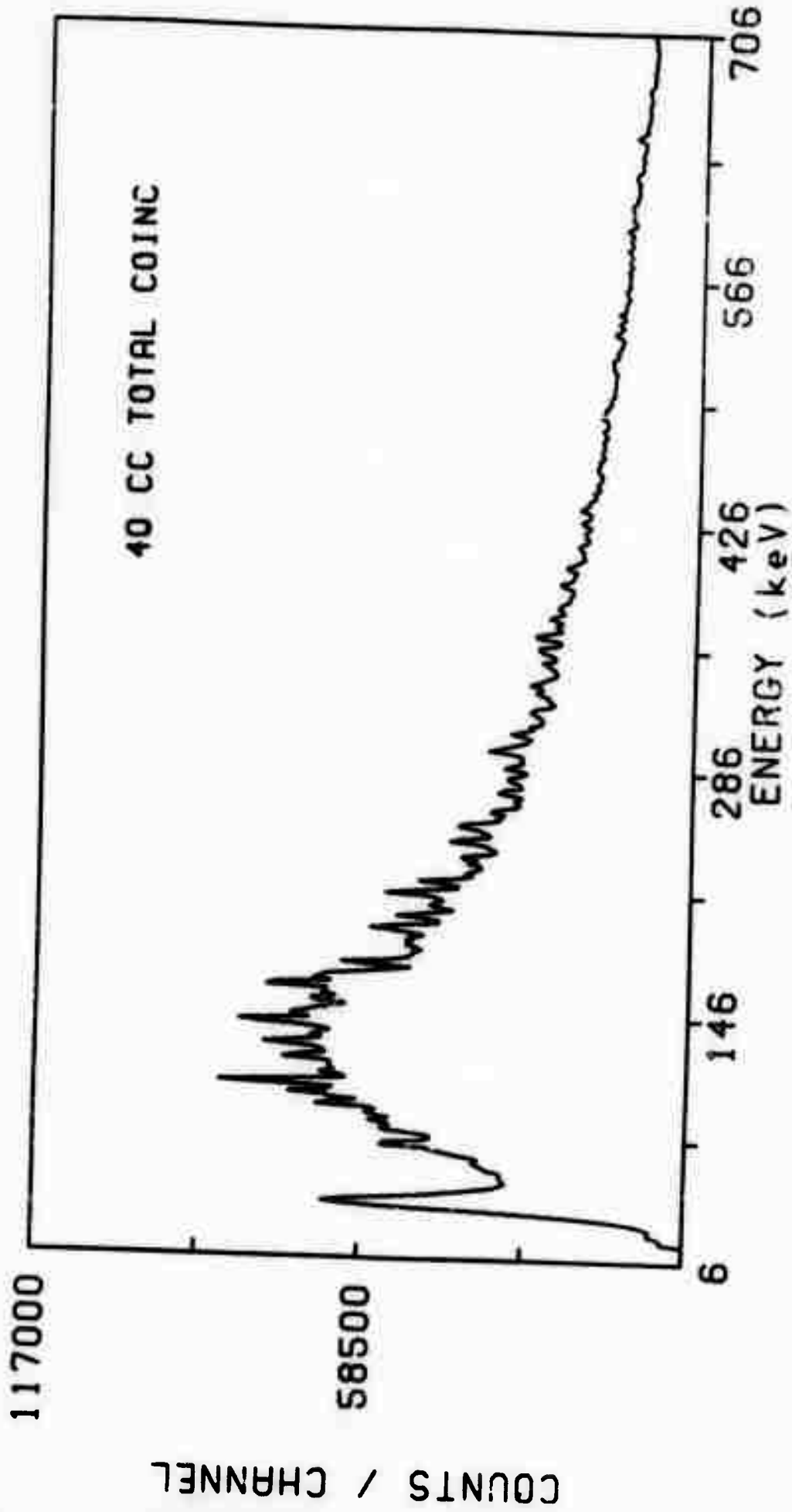
Fig. 12 Partial decay scheme for  $^{109}\text{Ru}$ .

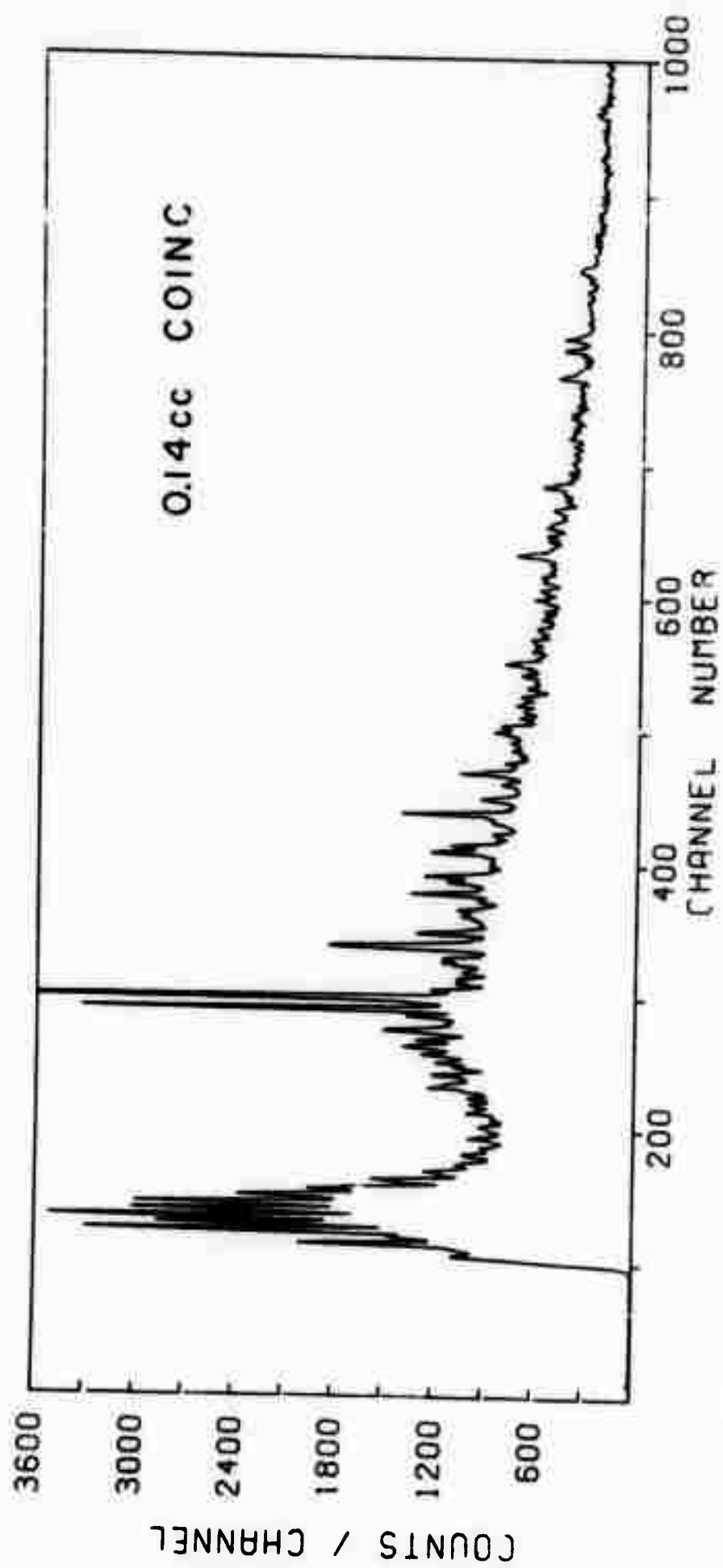


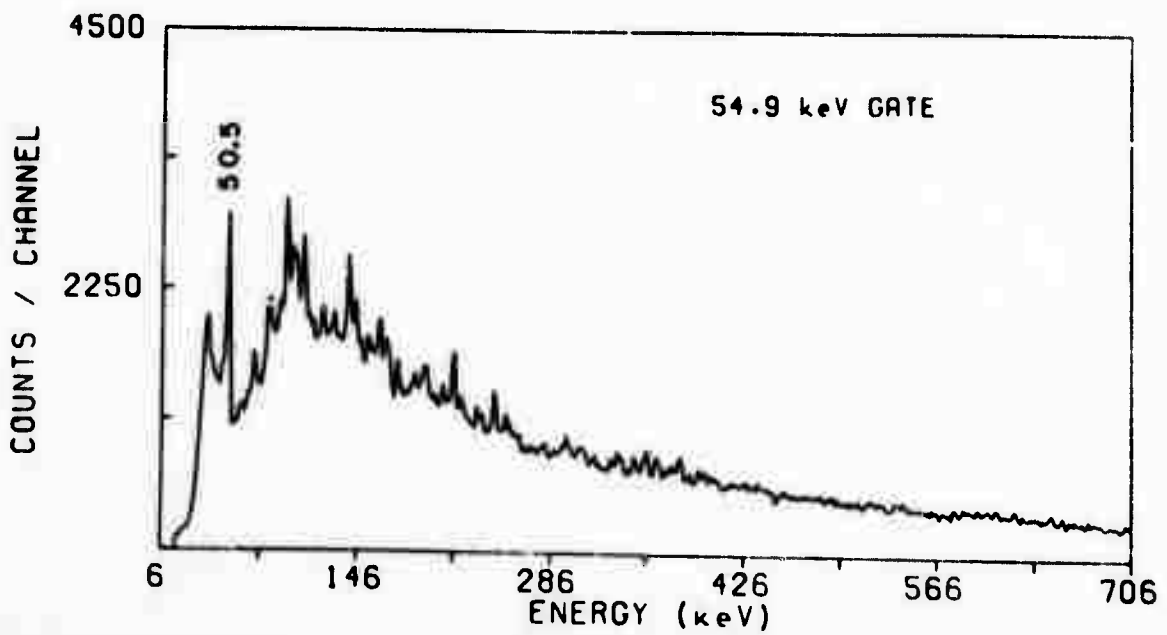
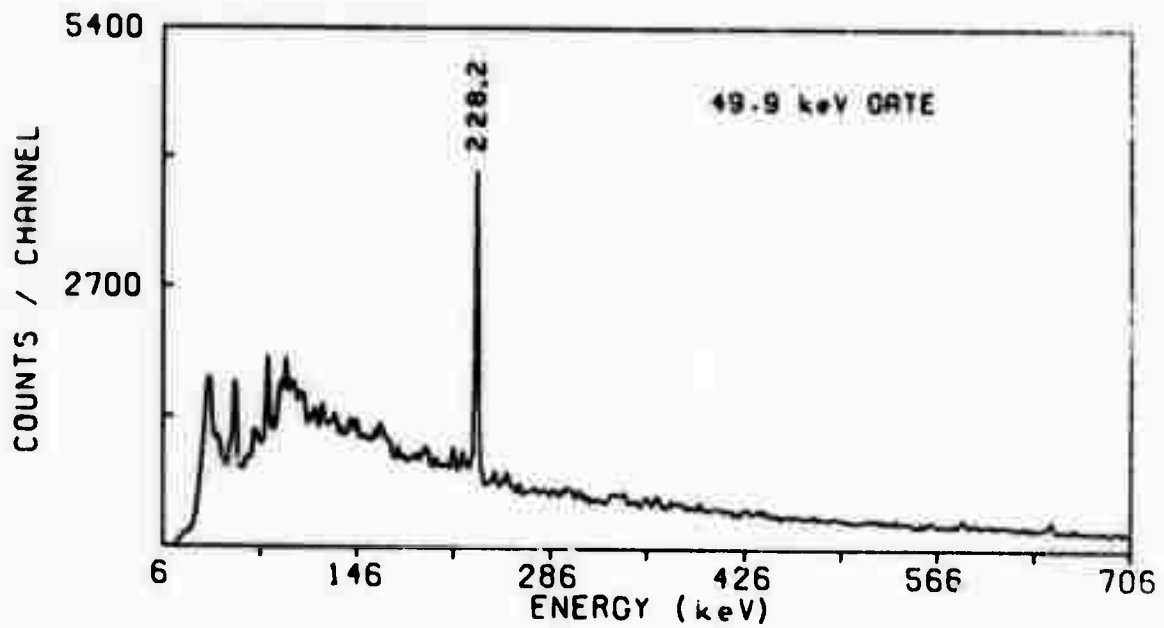
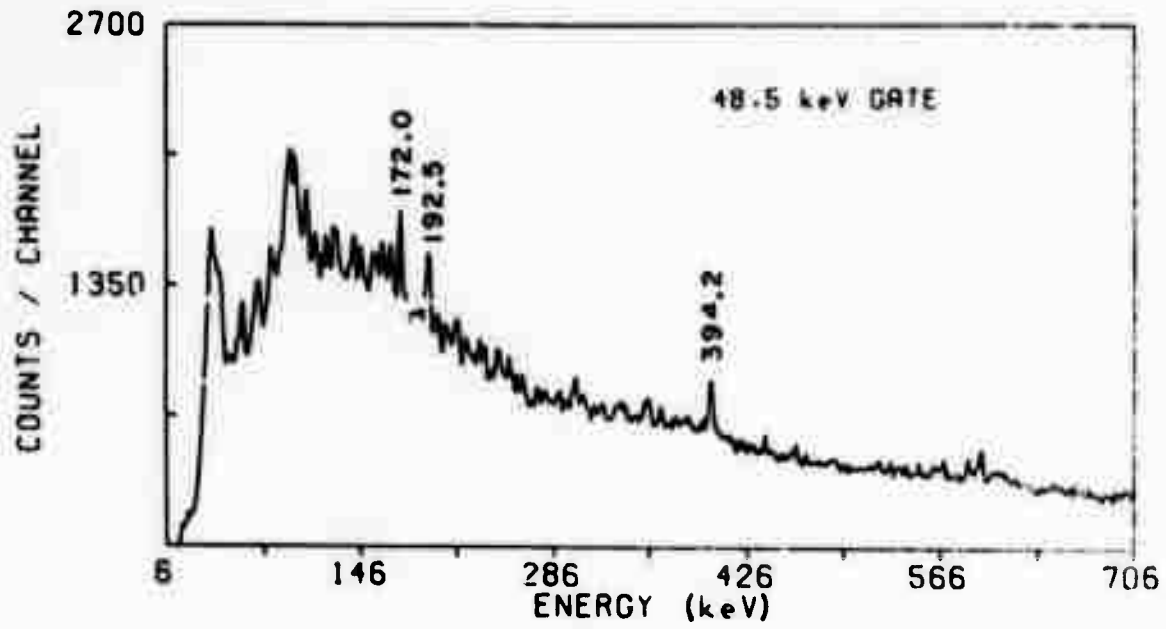
# EXPERIMENTAL SETUP

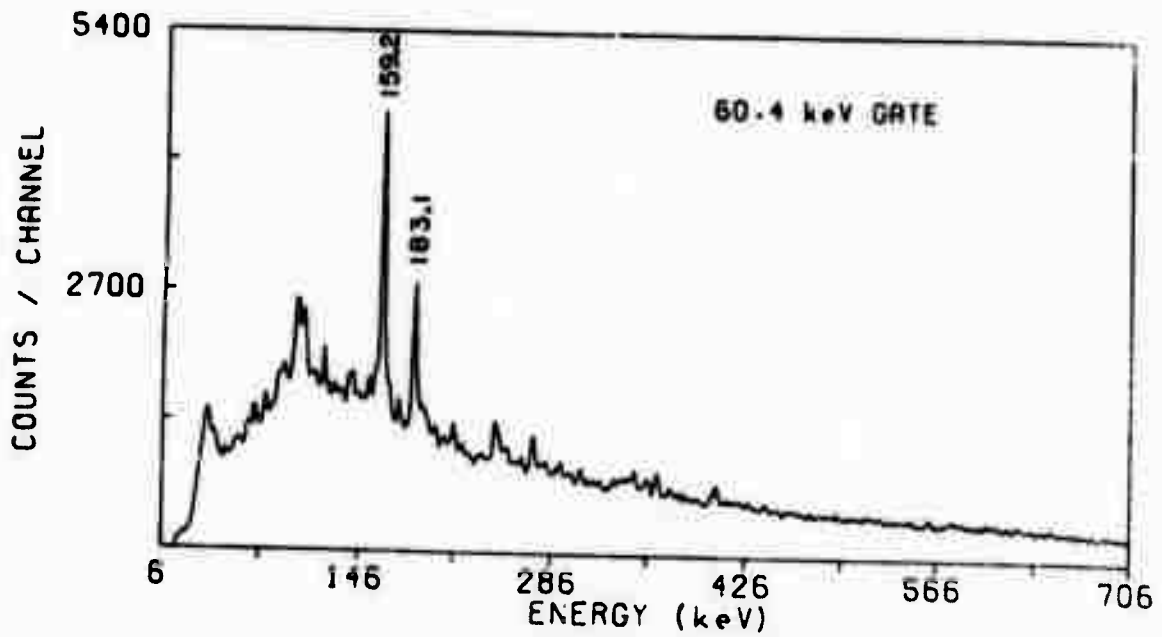
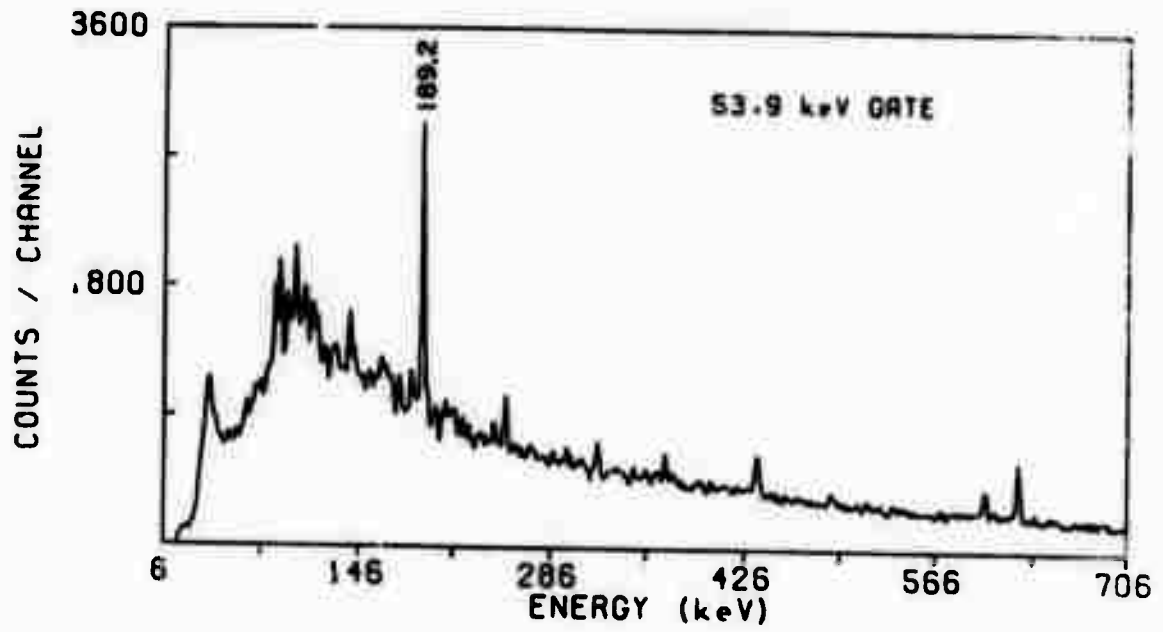
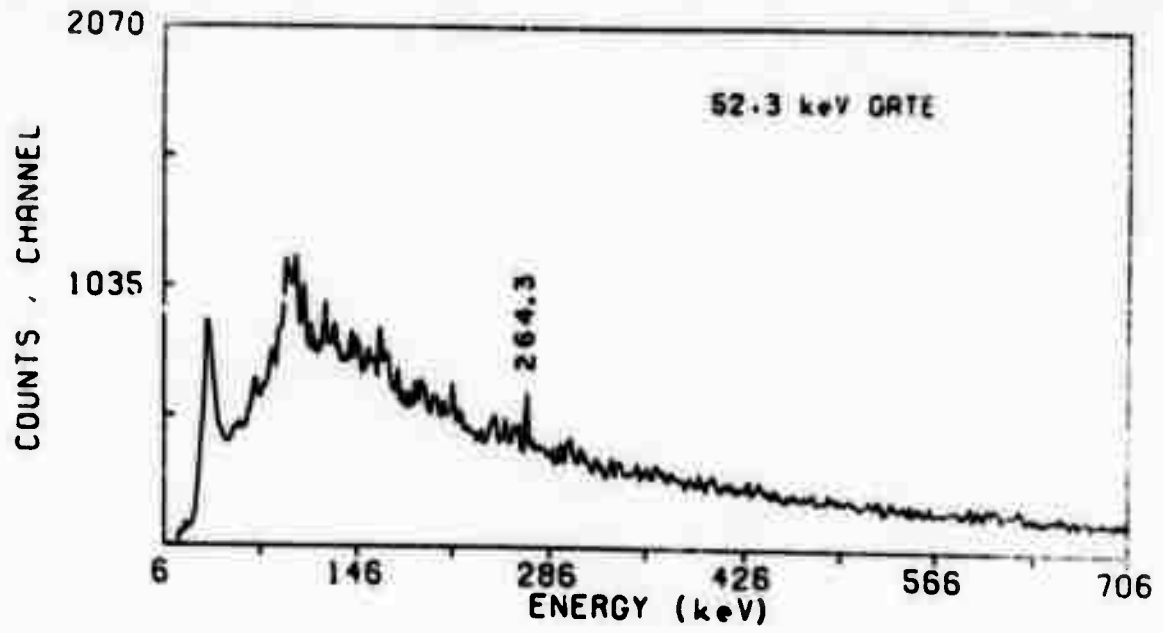


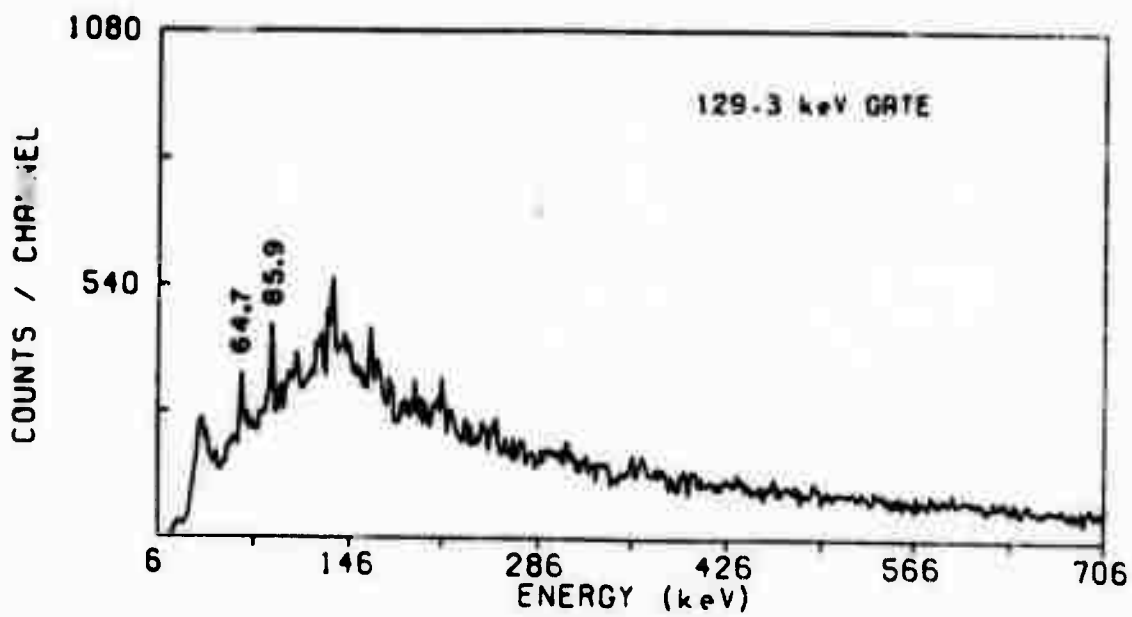
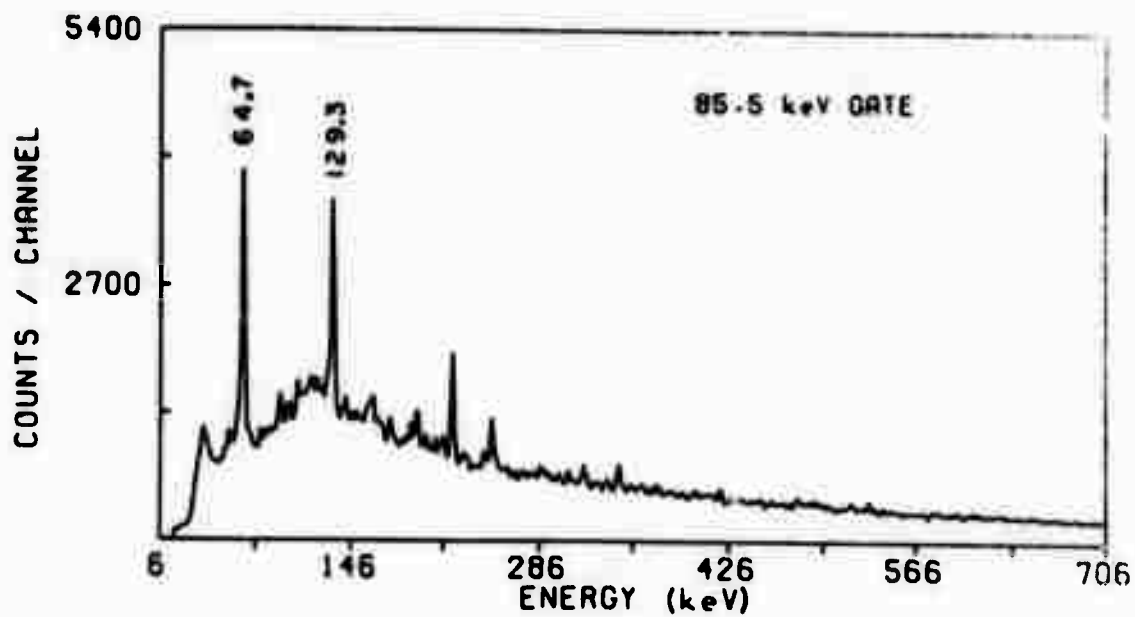
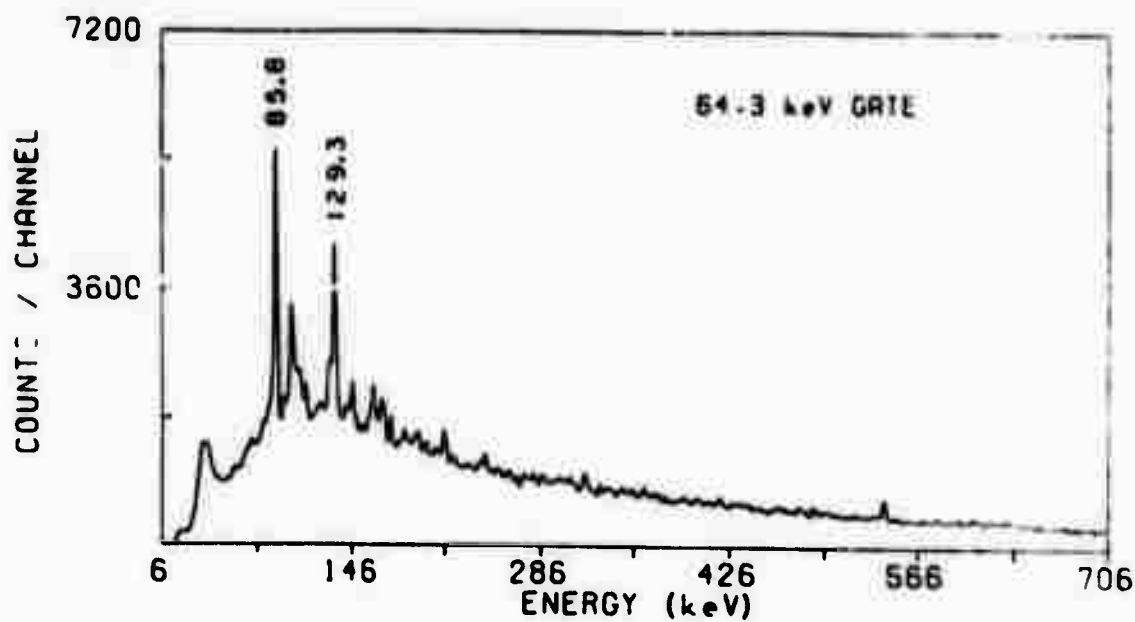


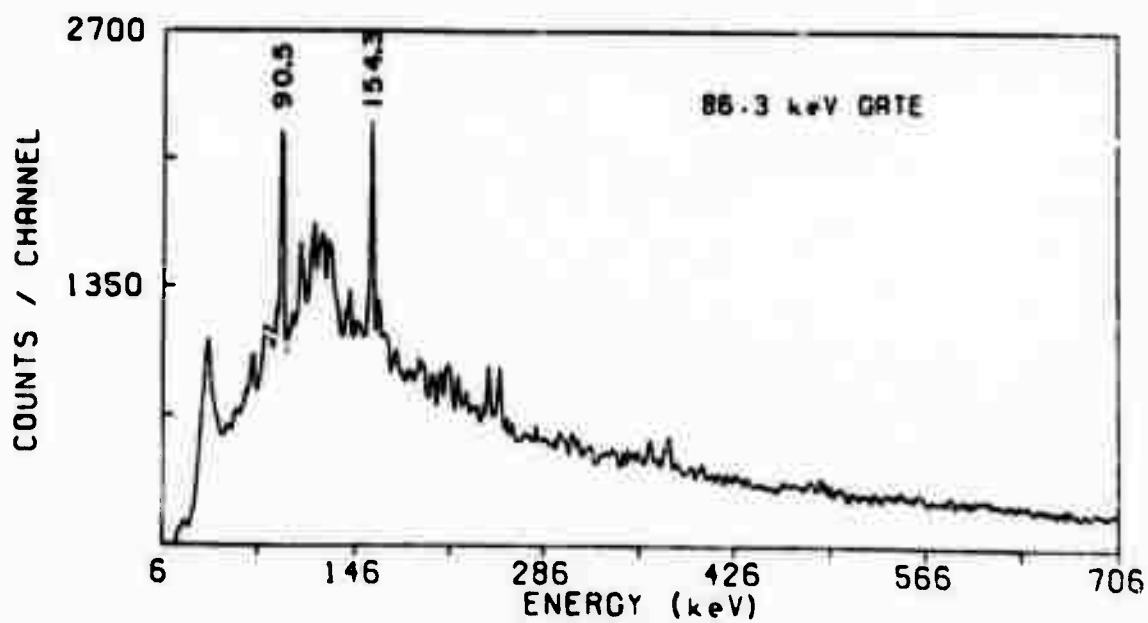
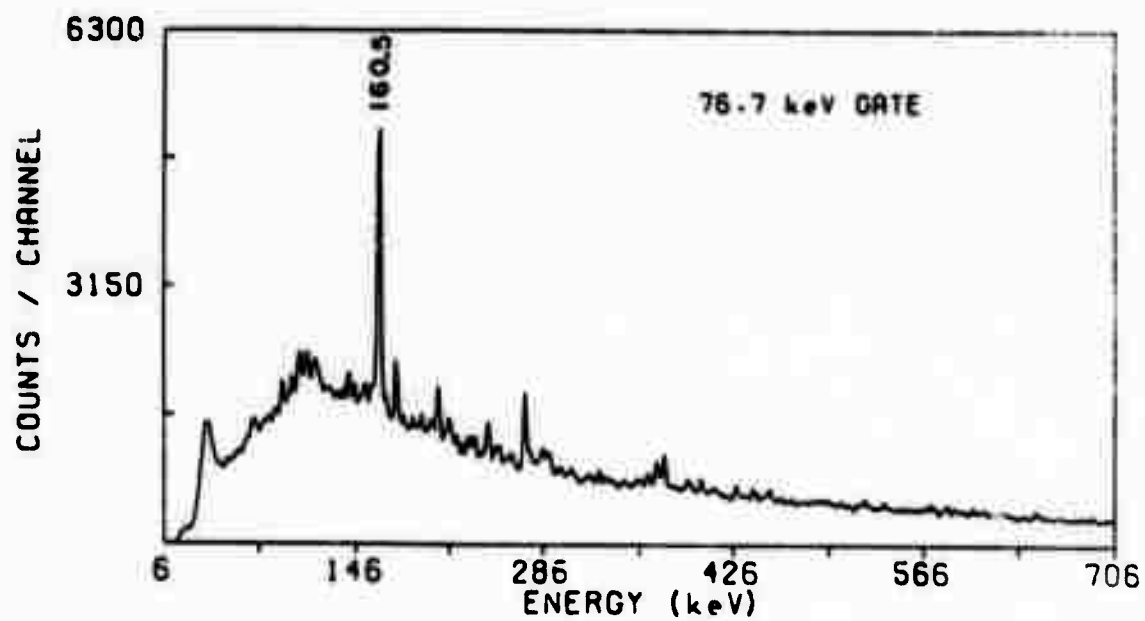
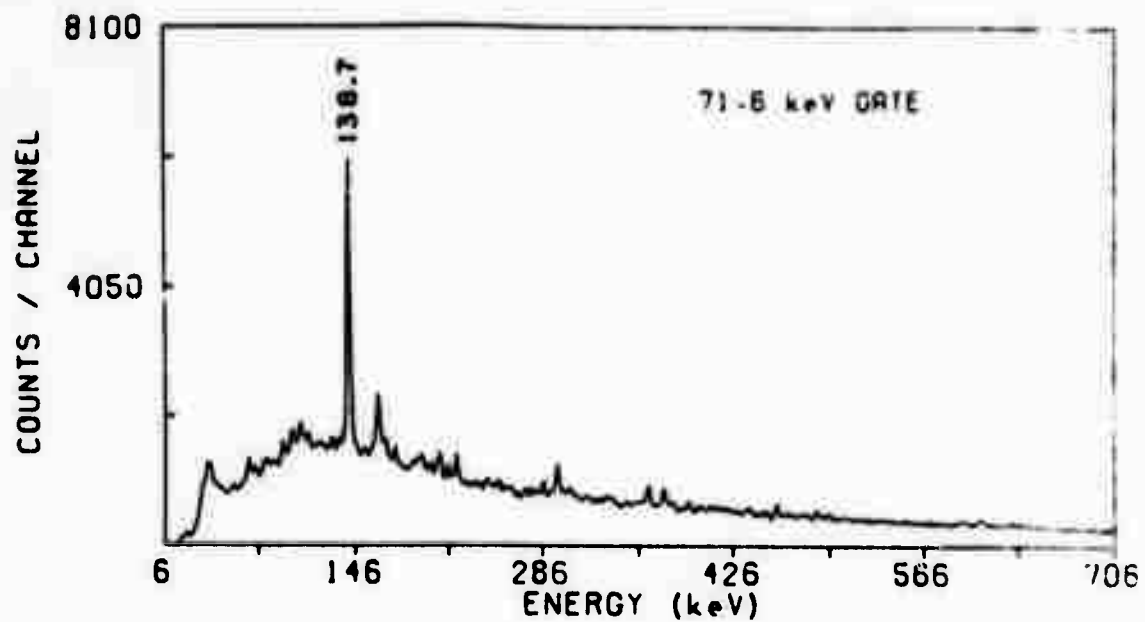


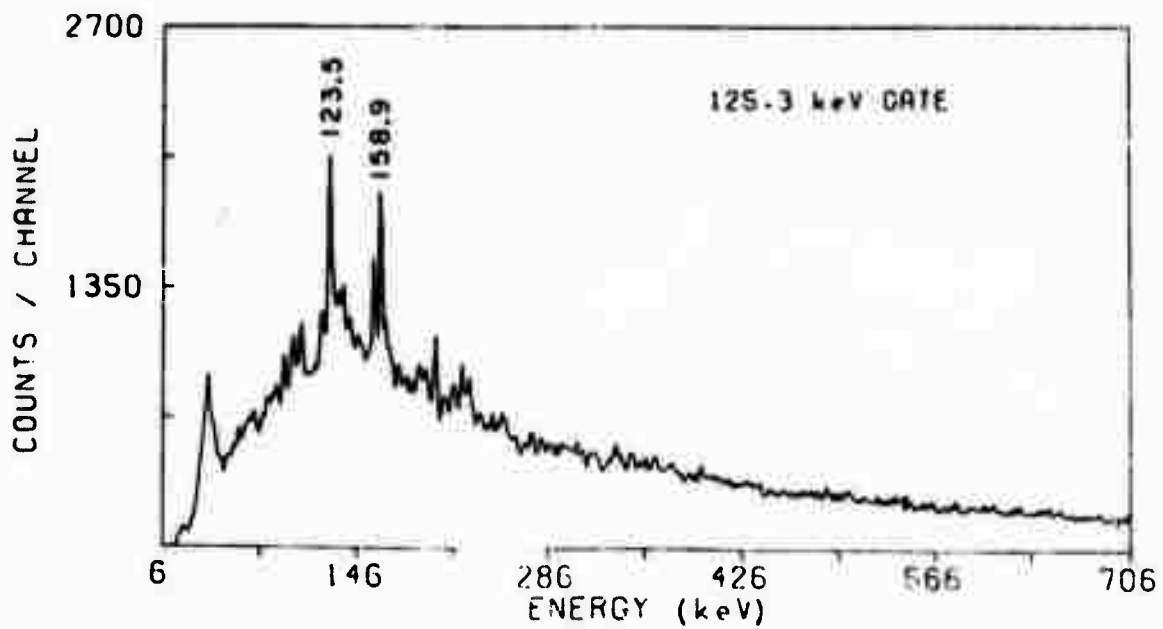
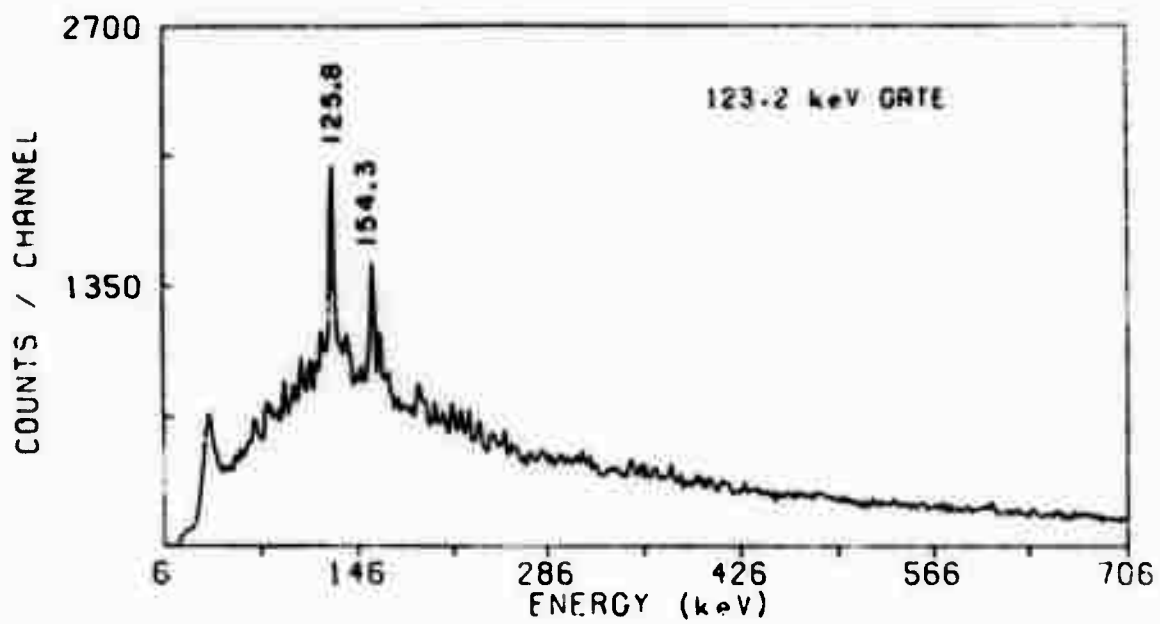
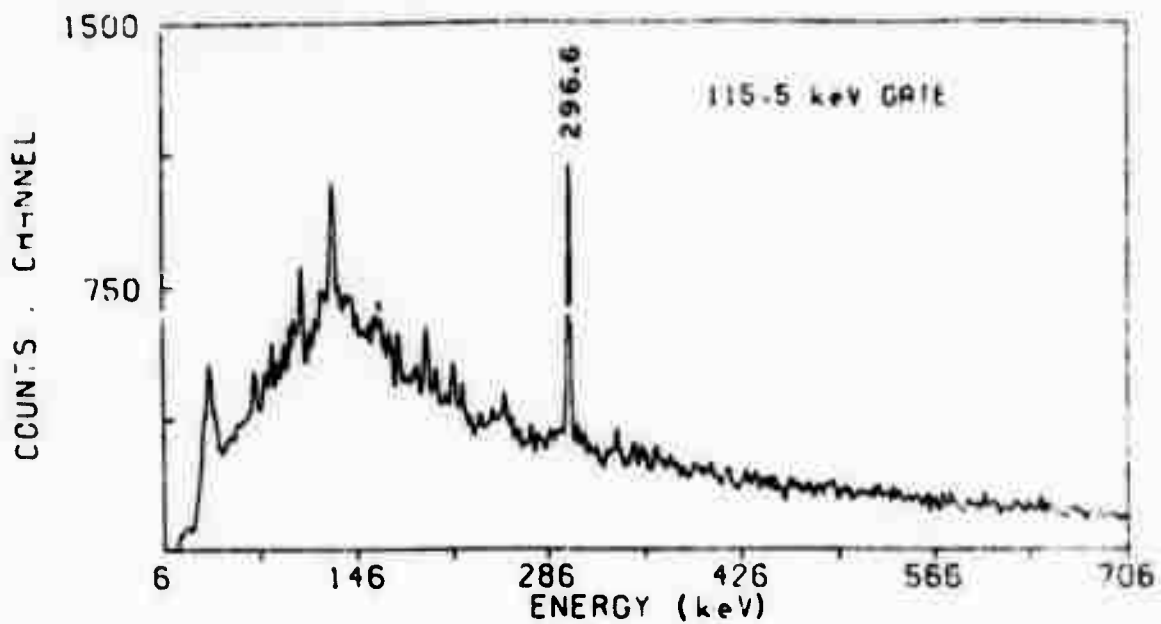


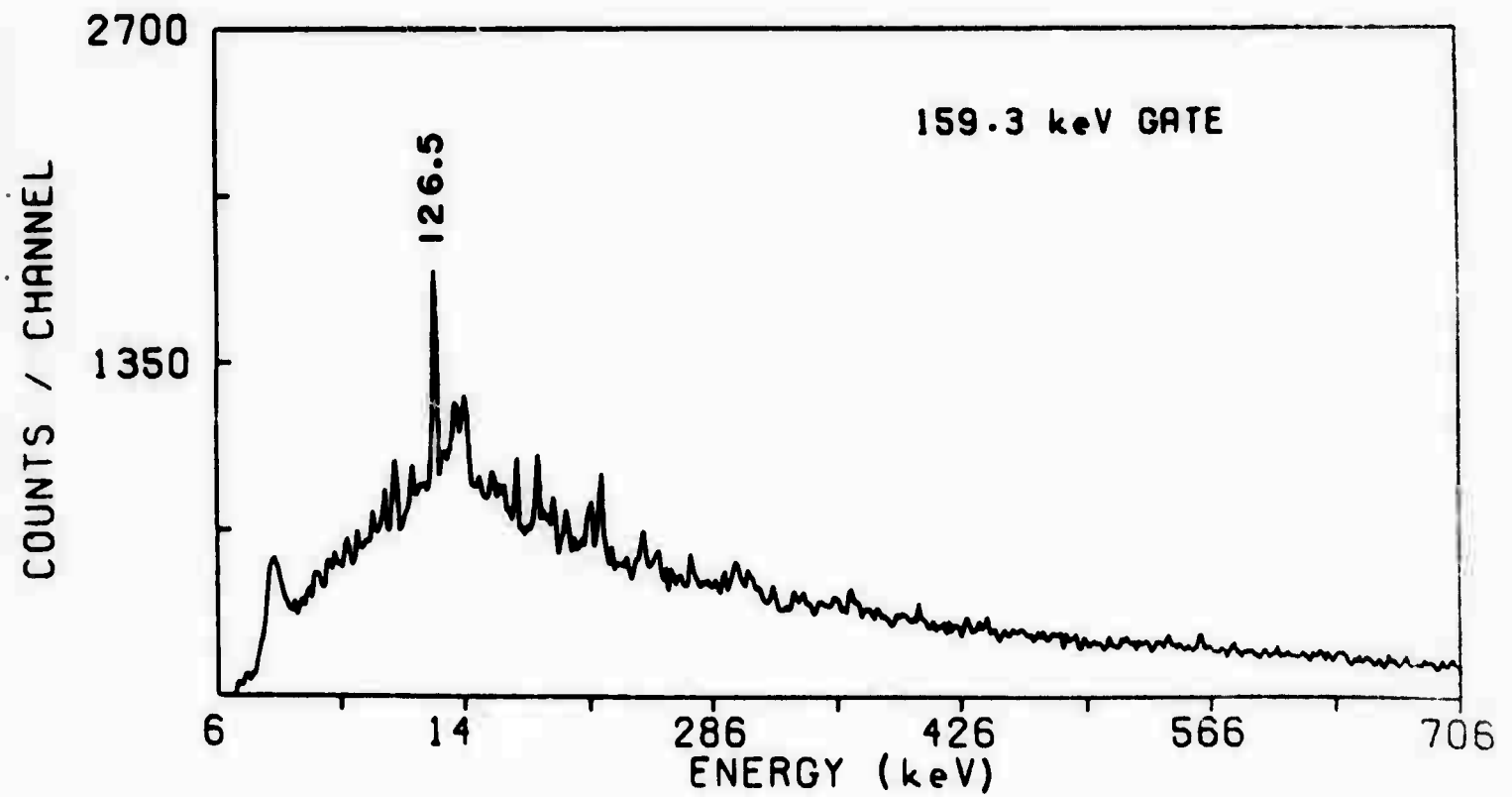
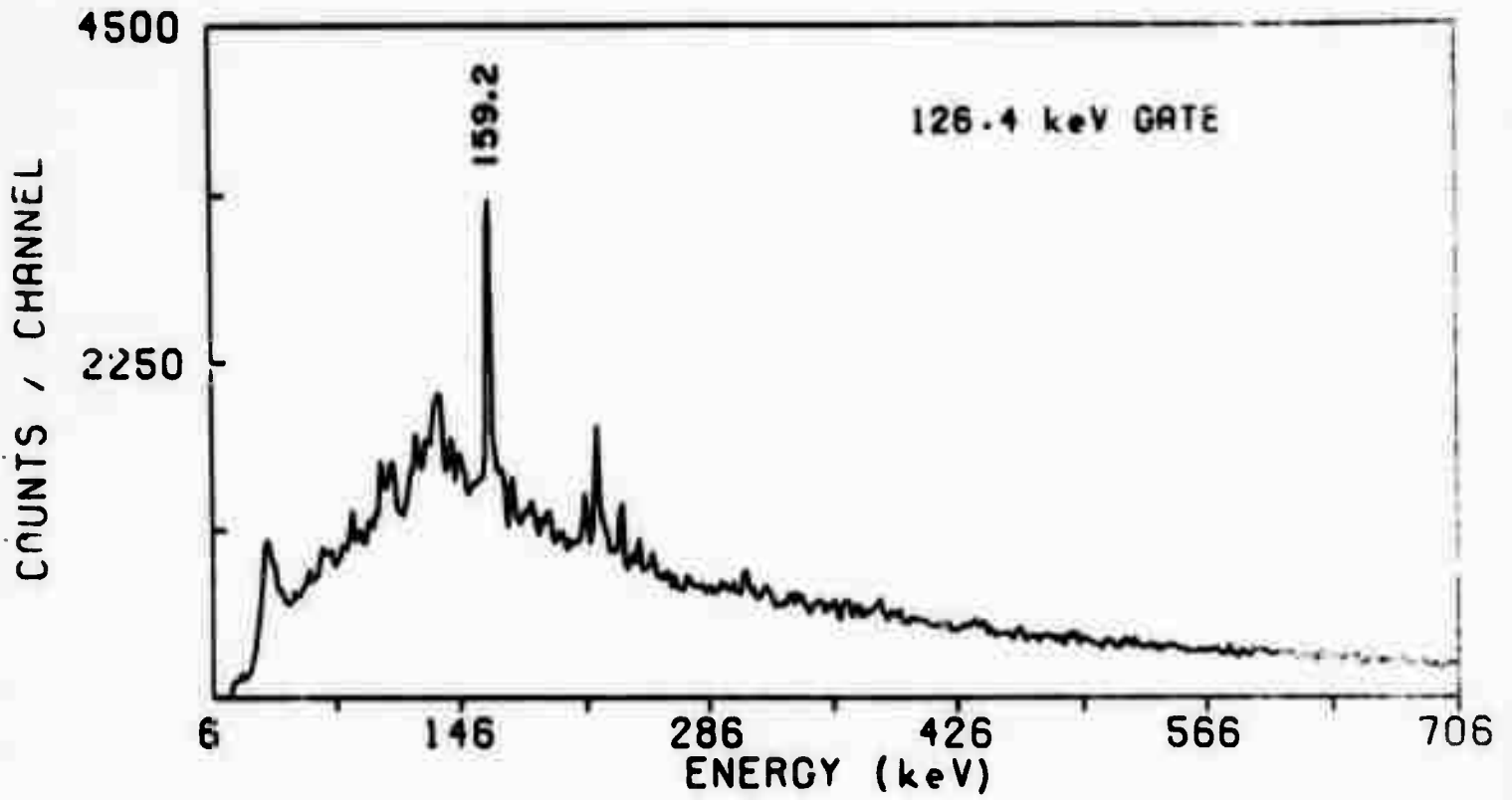


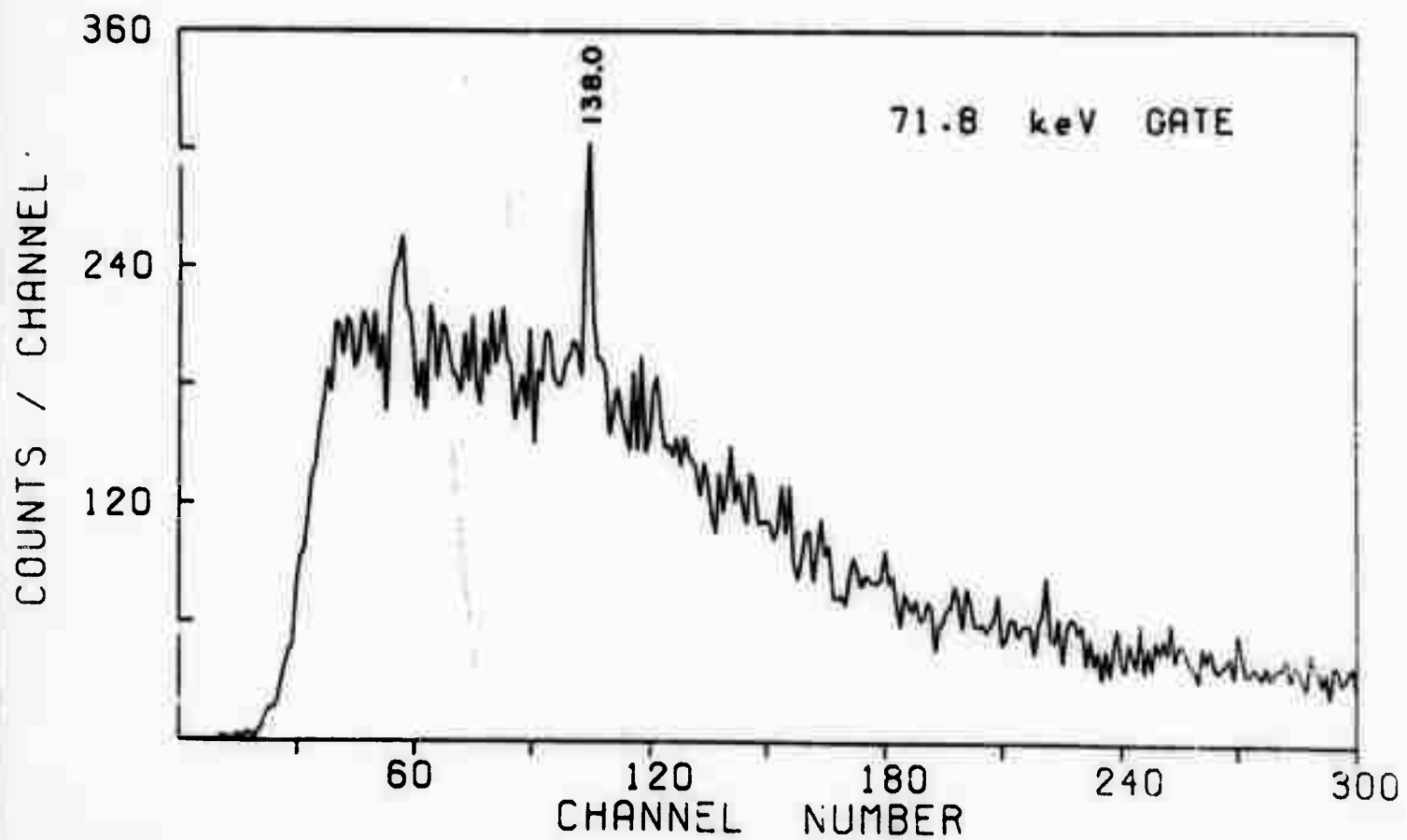
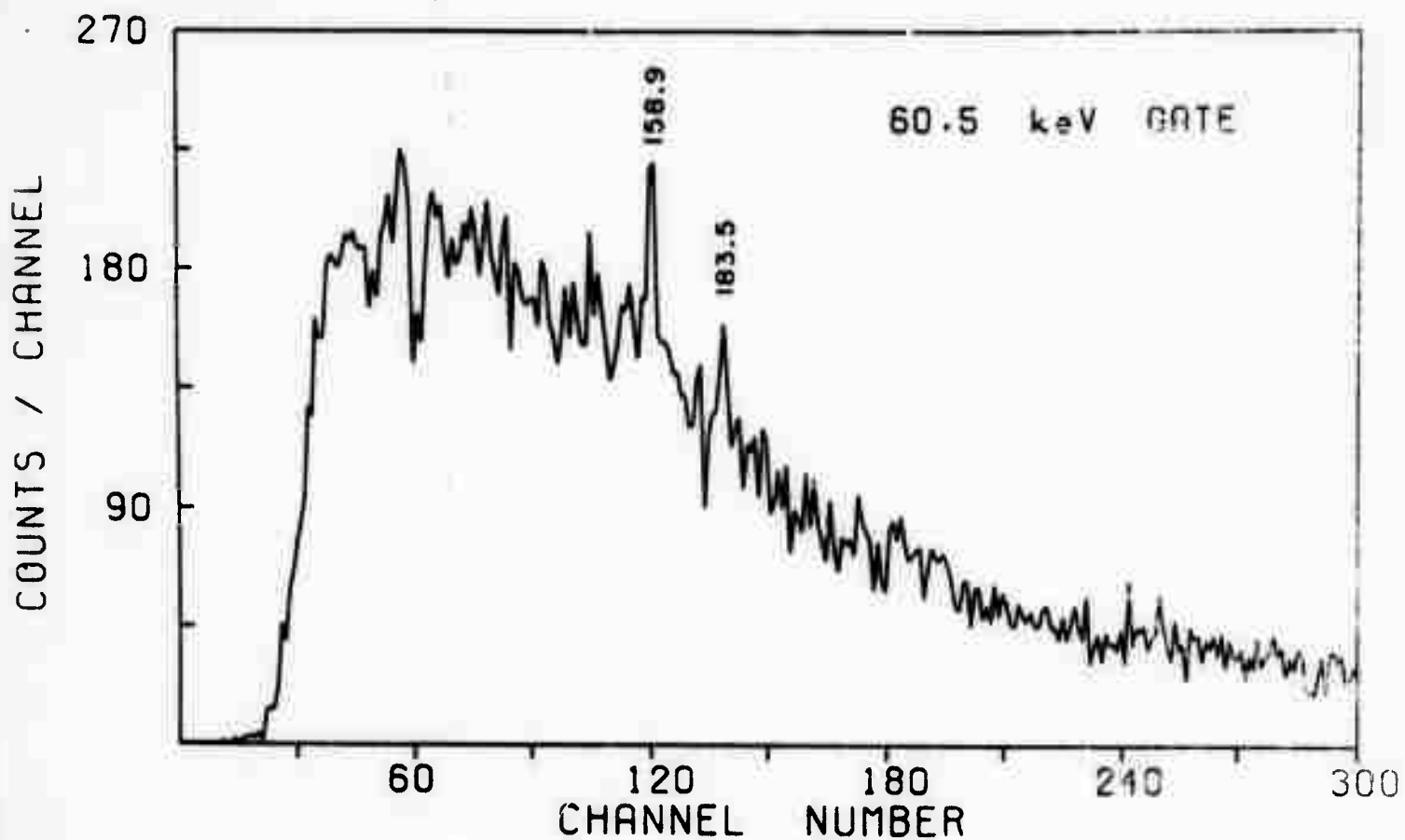


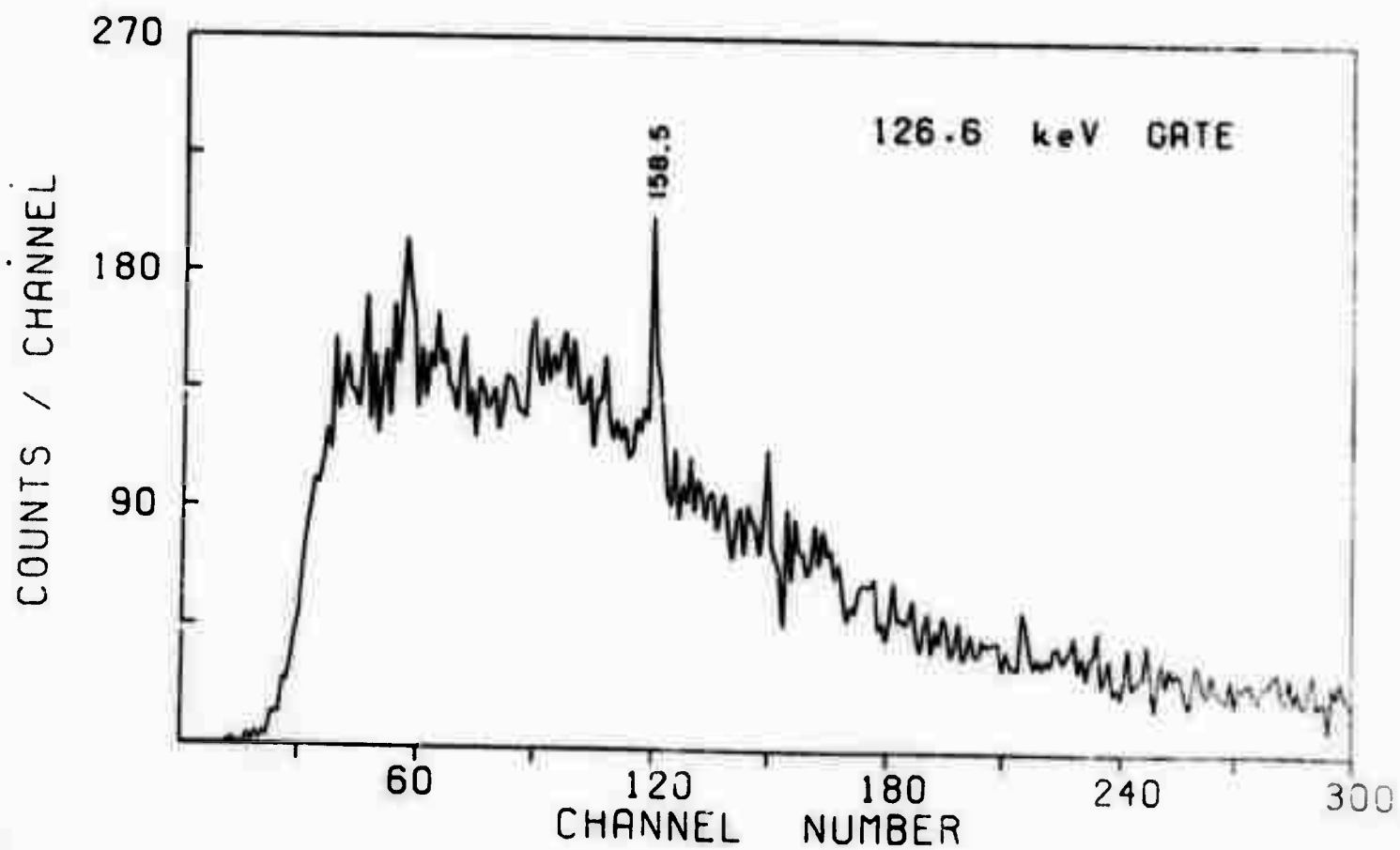
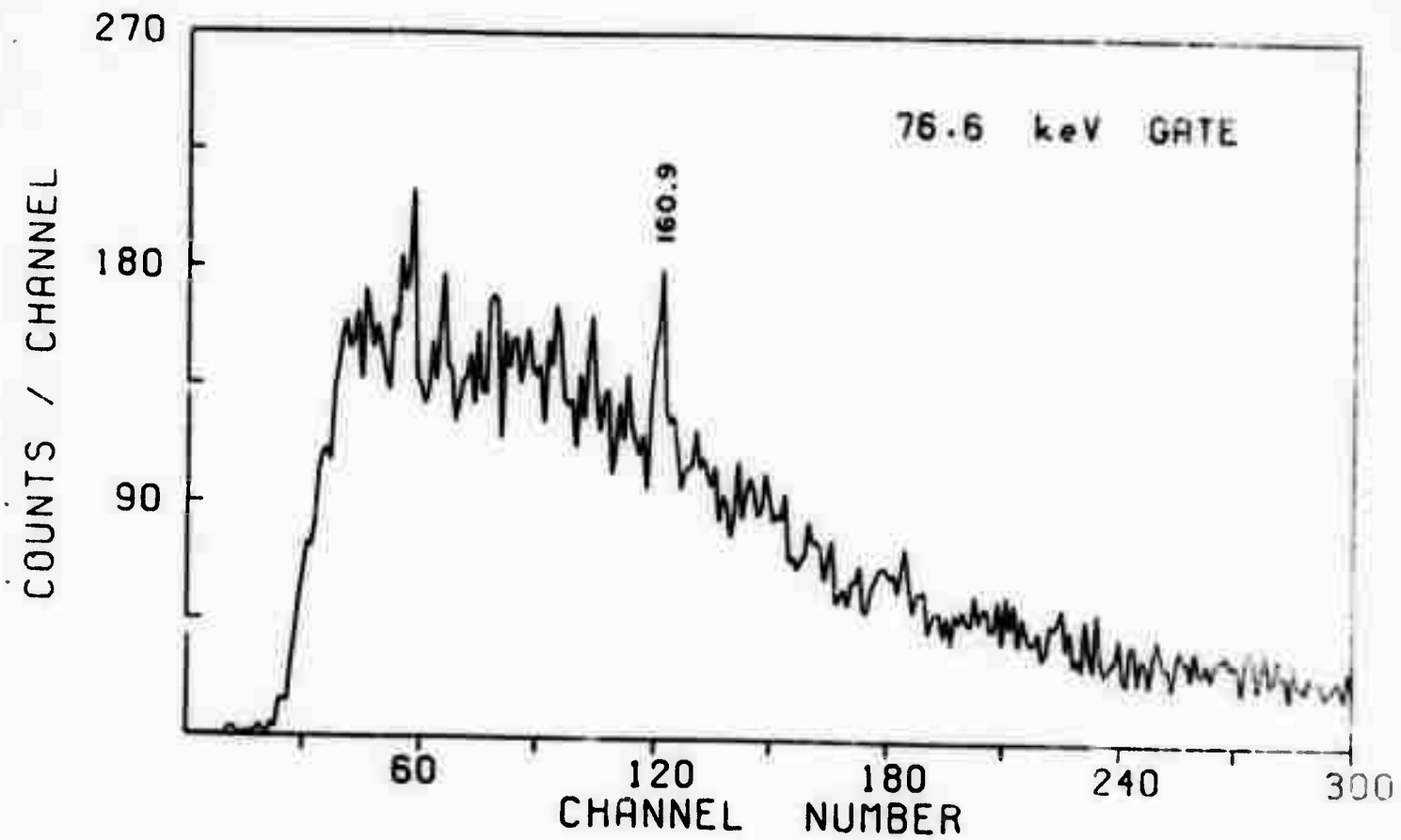


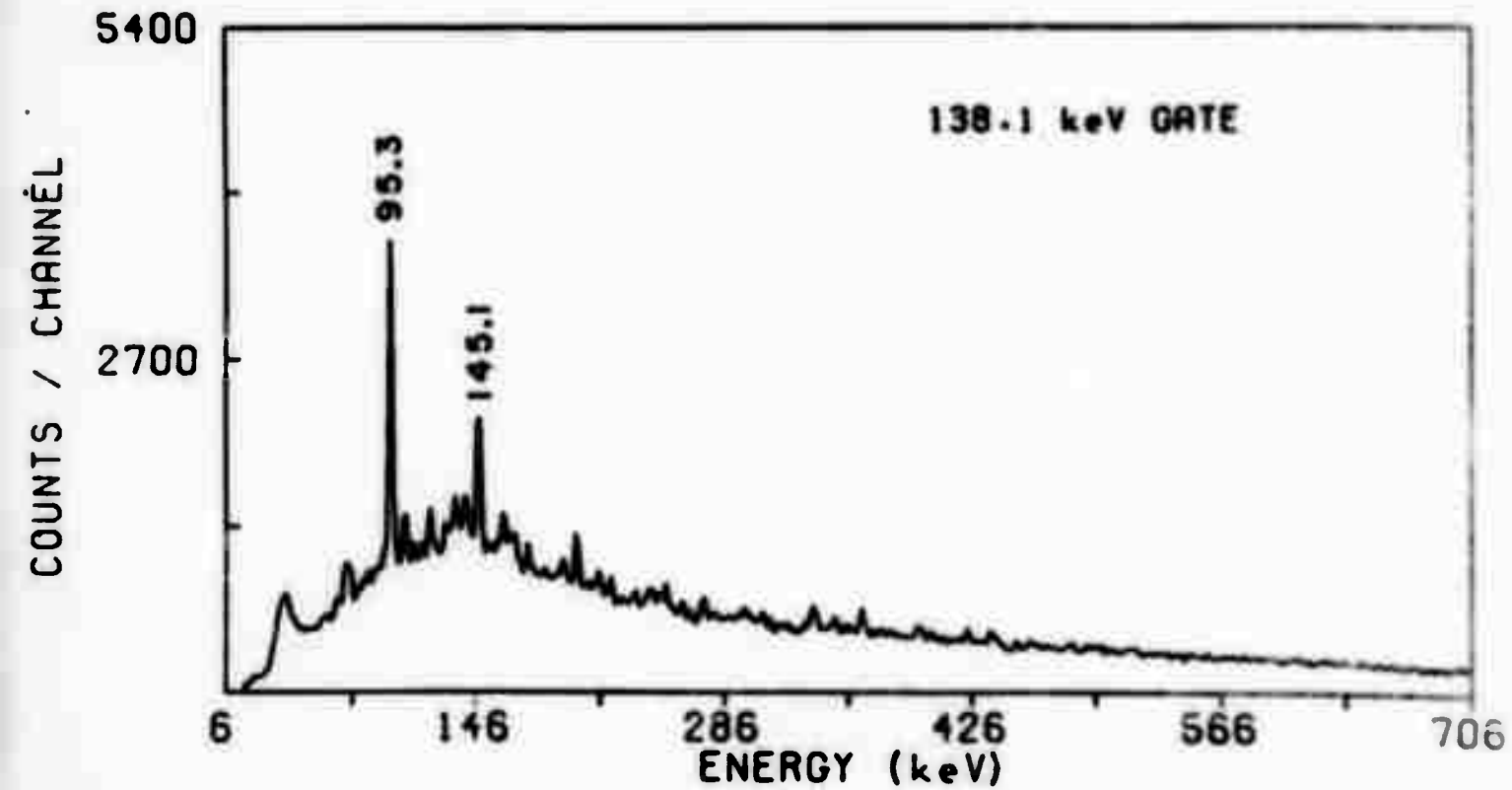
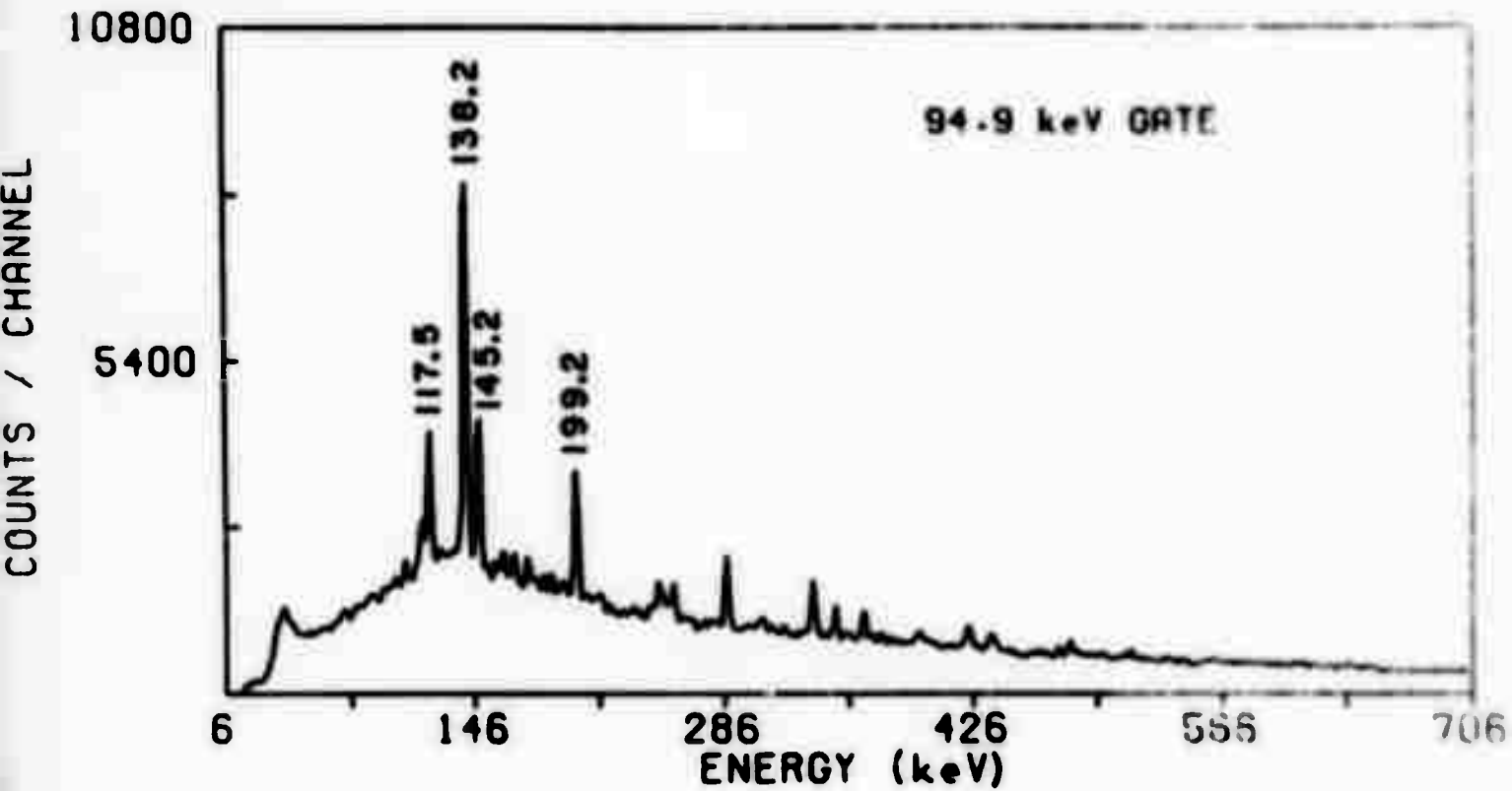


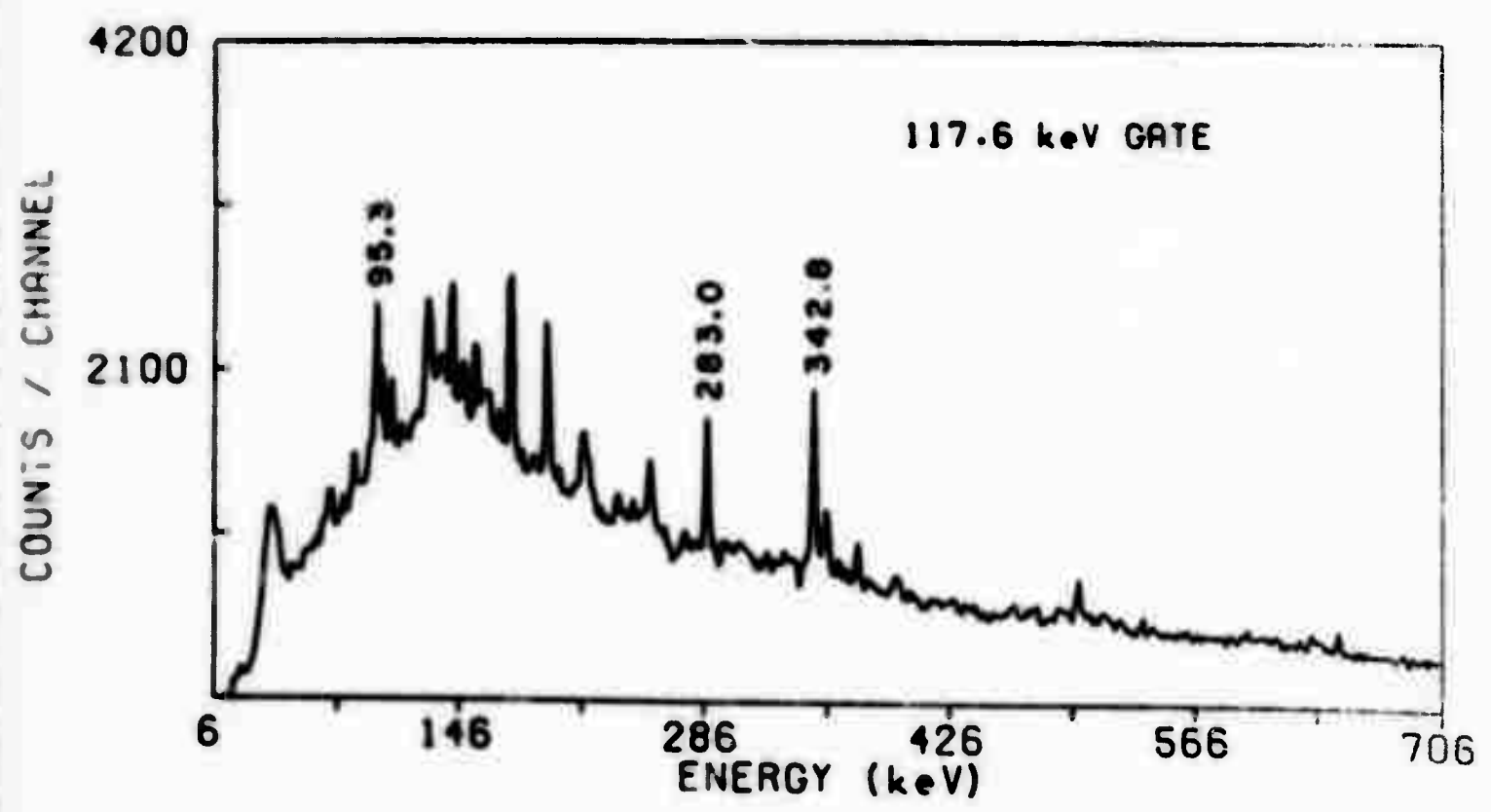
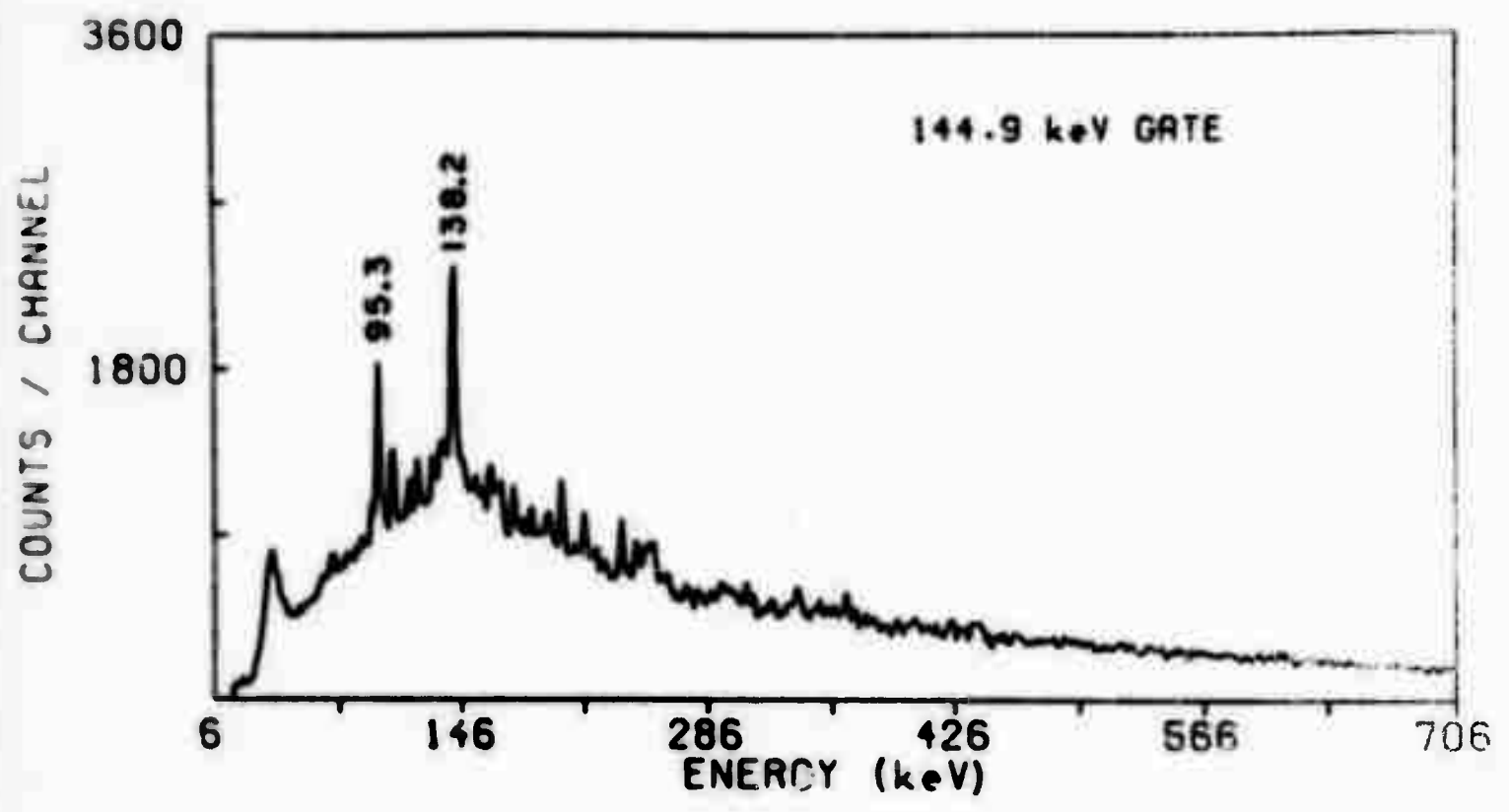


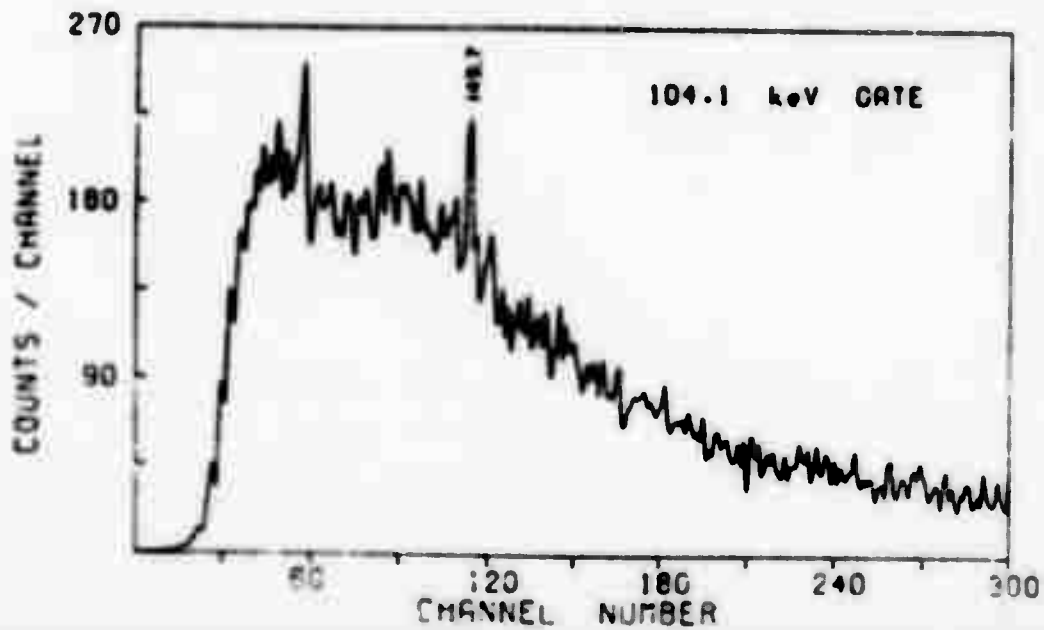
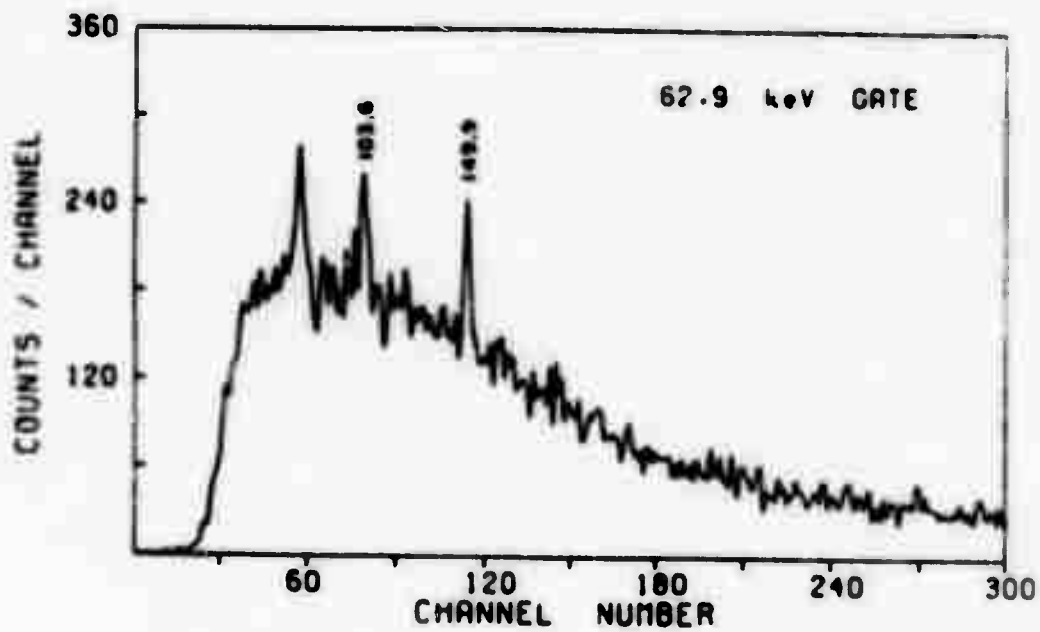
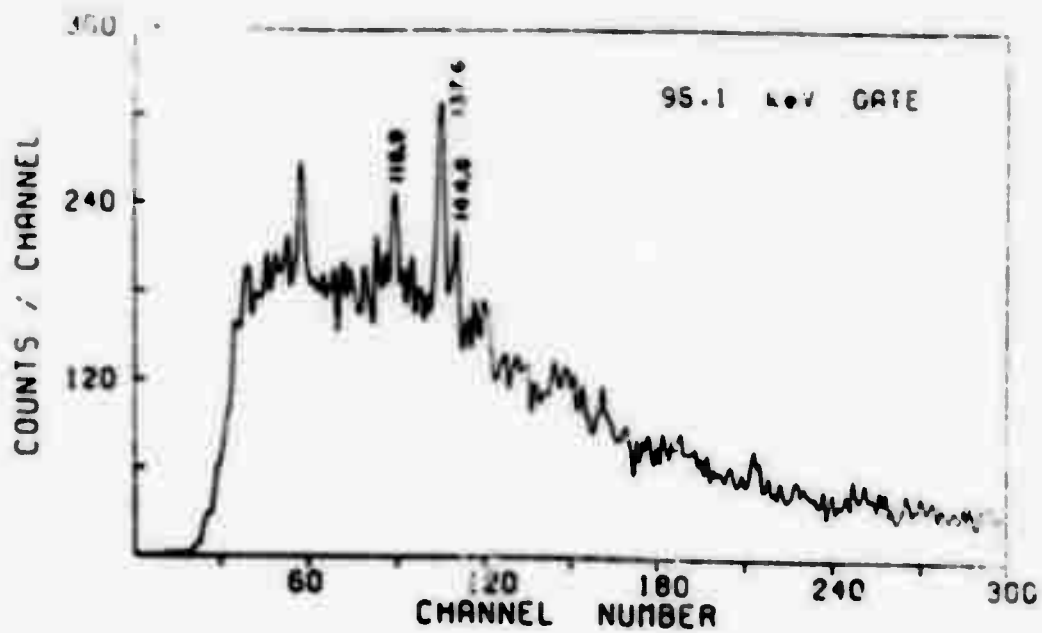


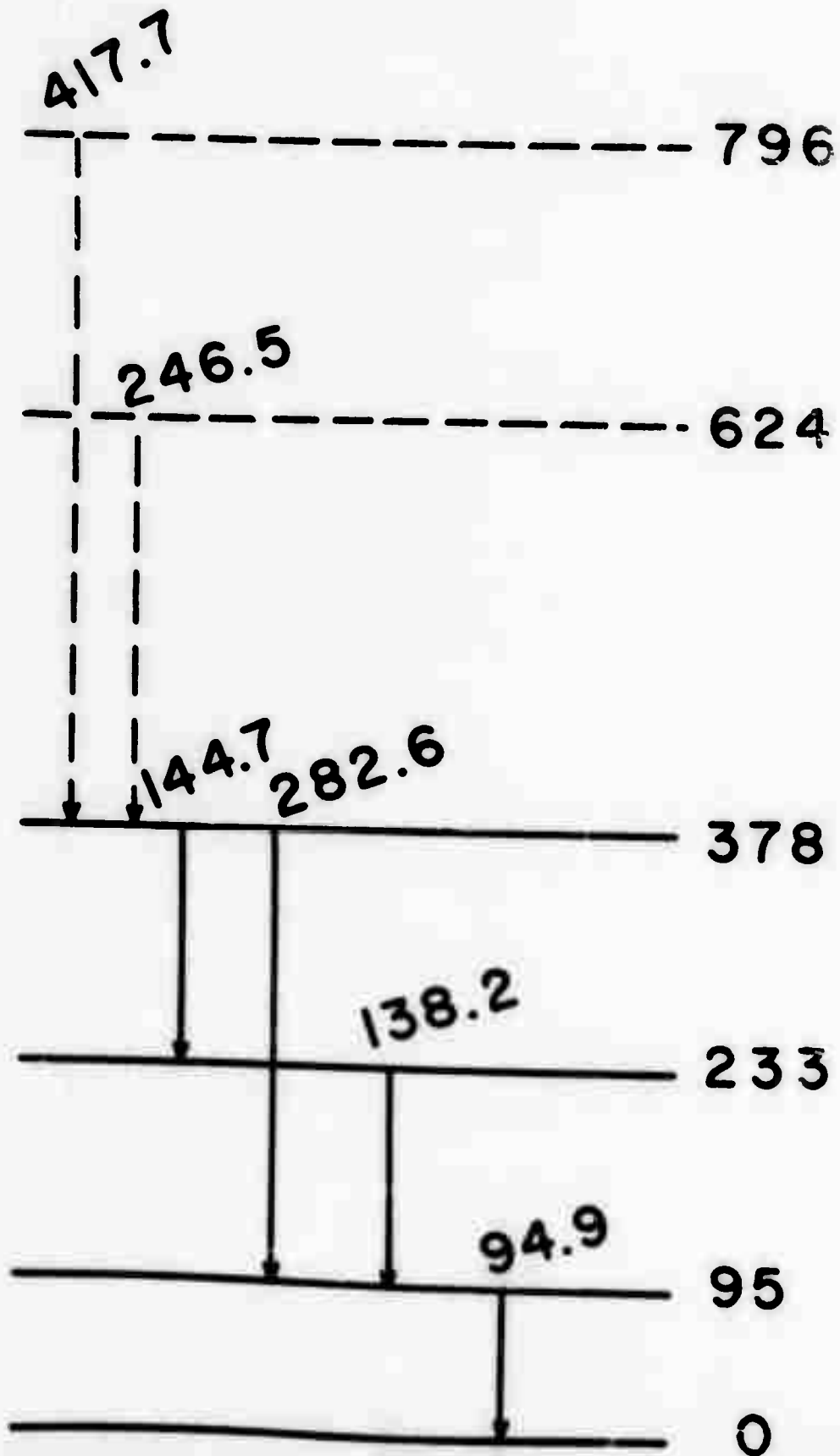


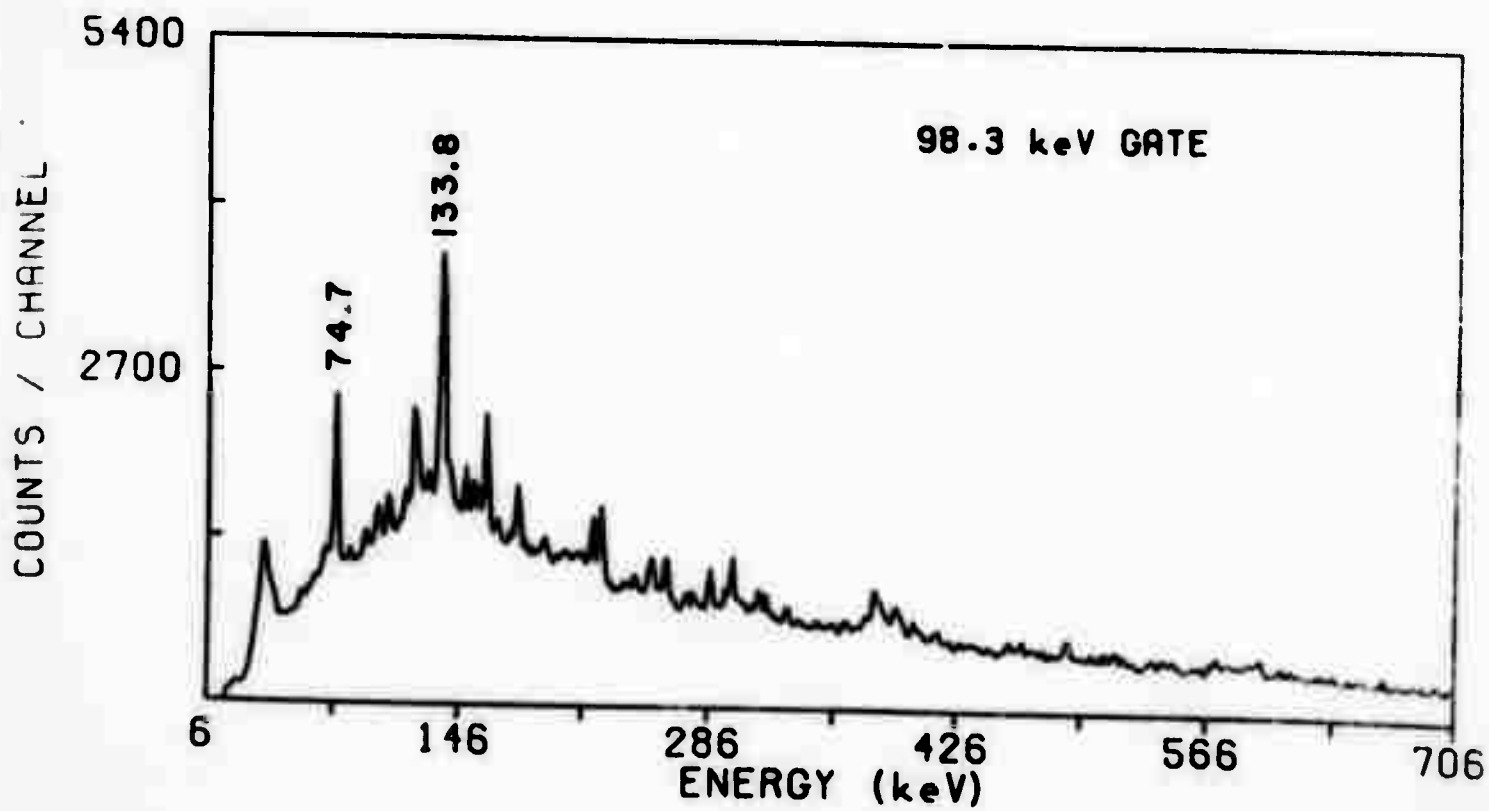
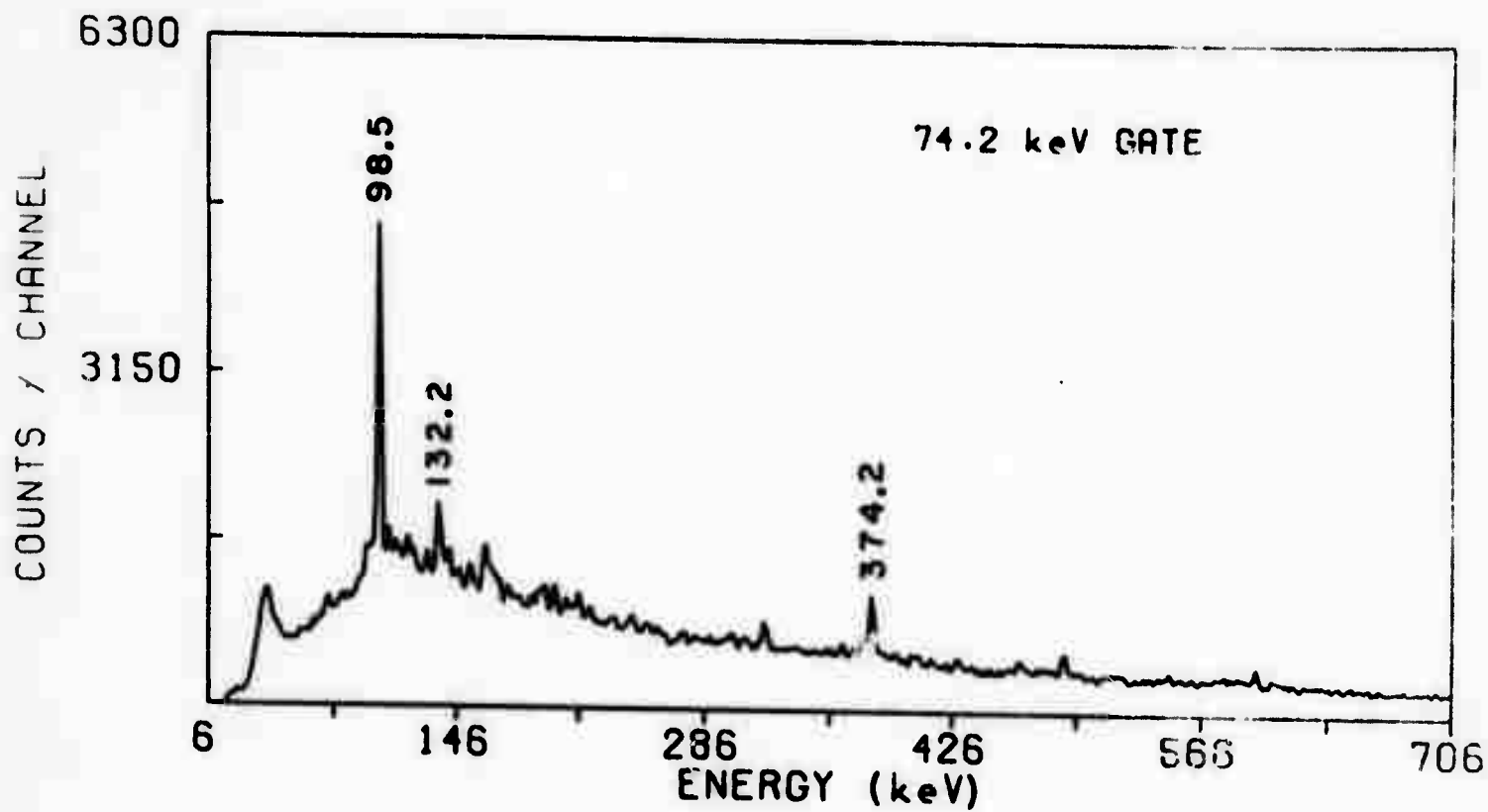


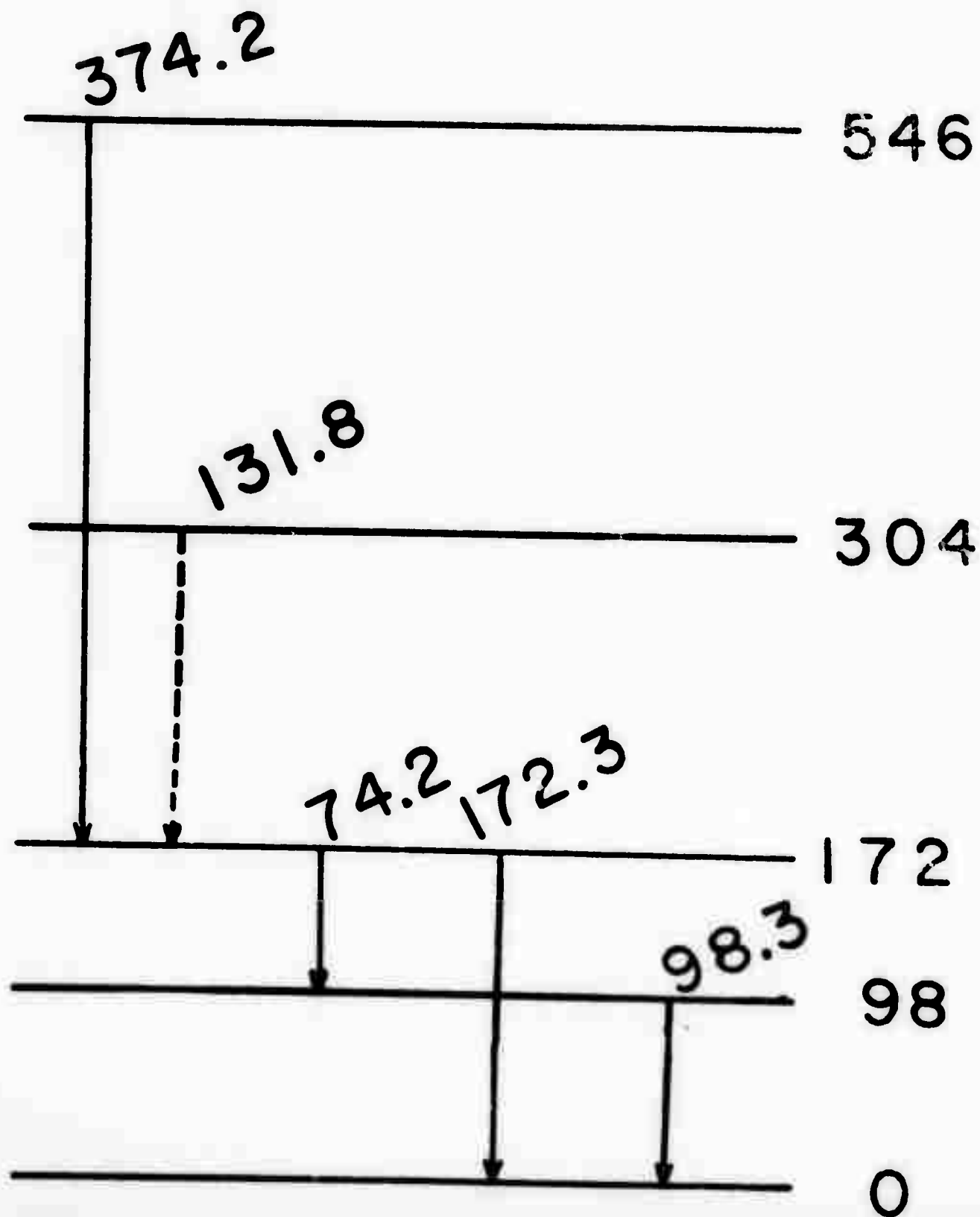


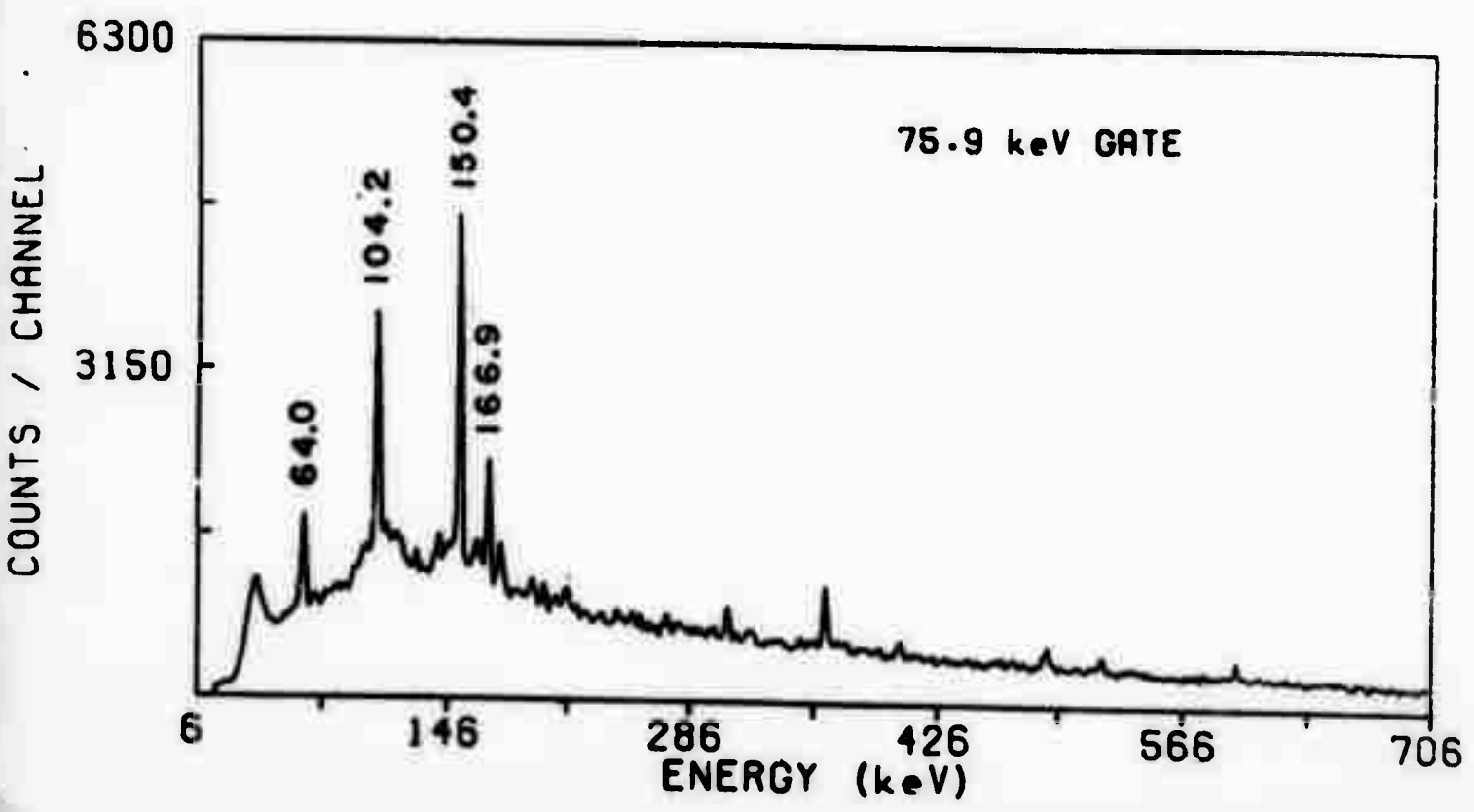
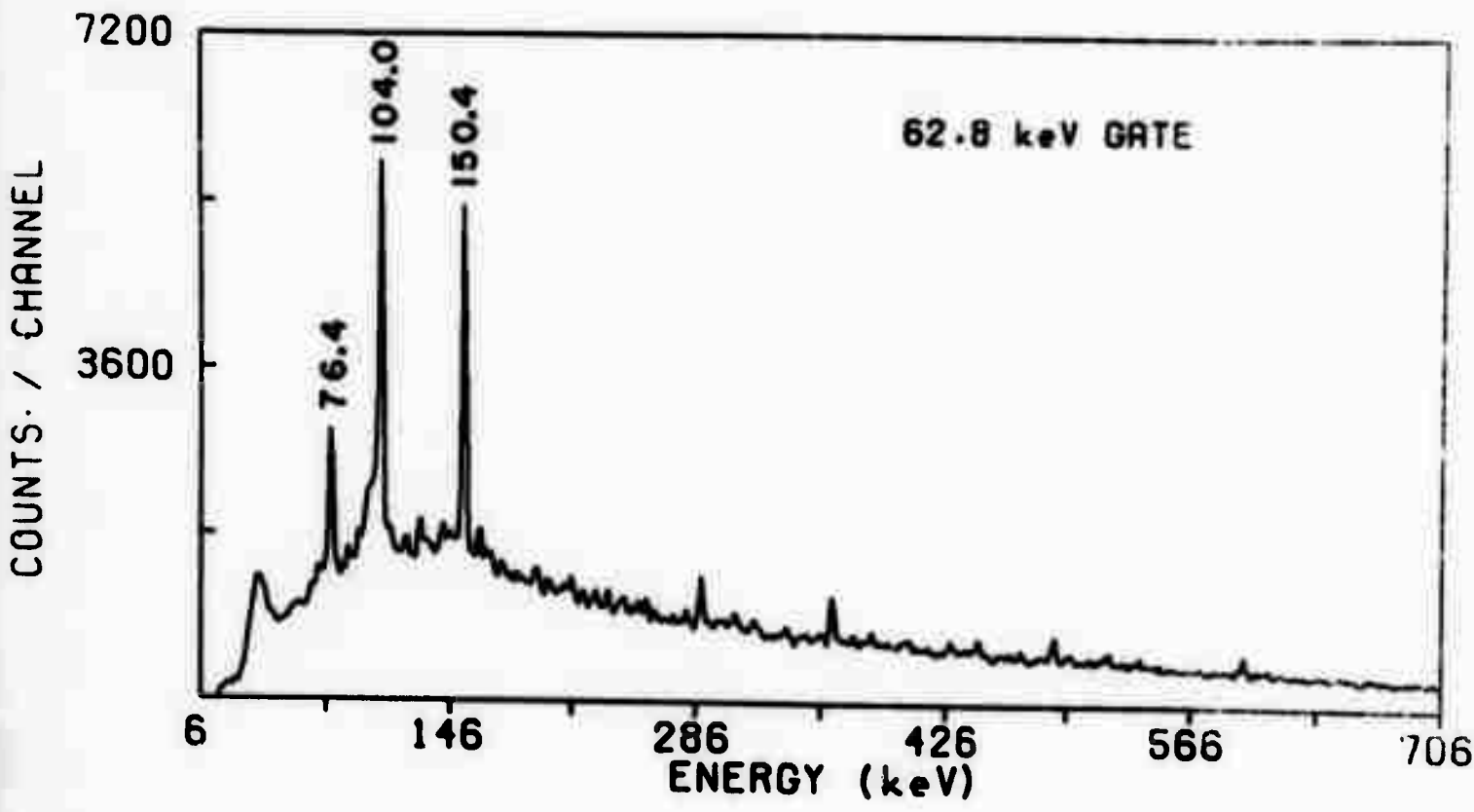


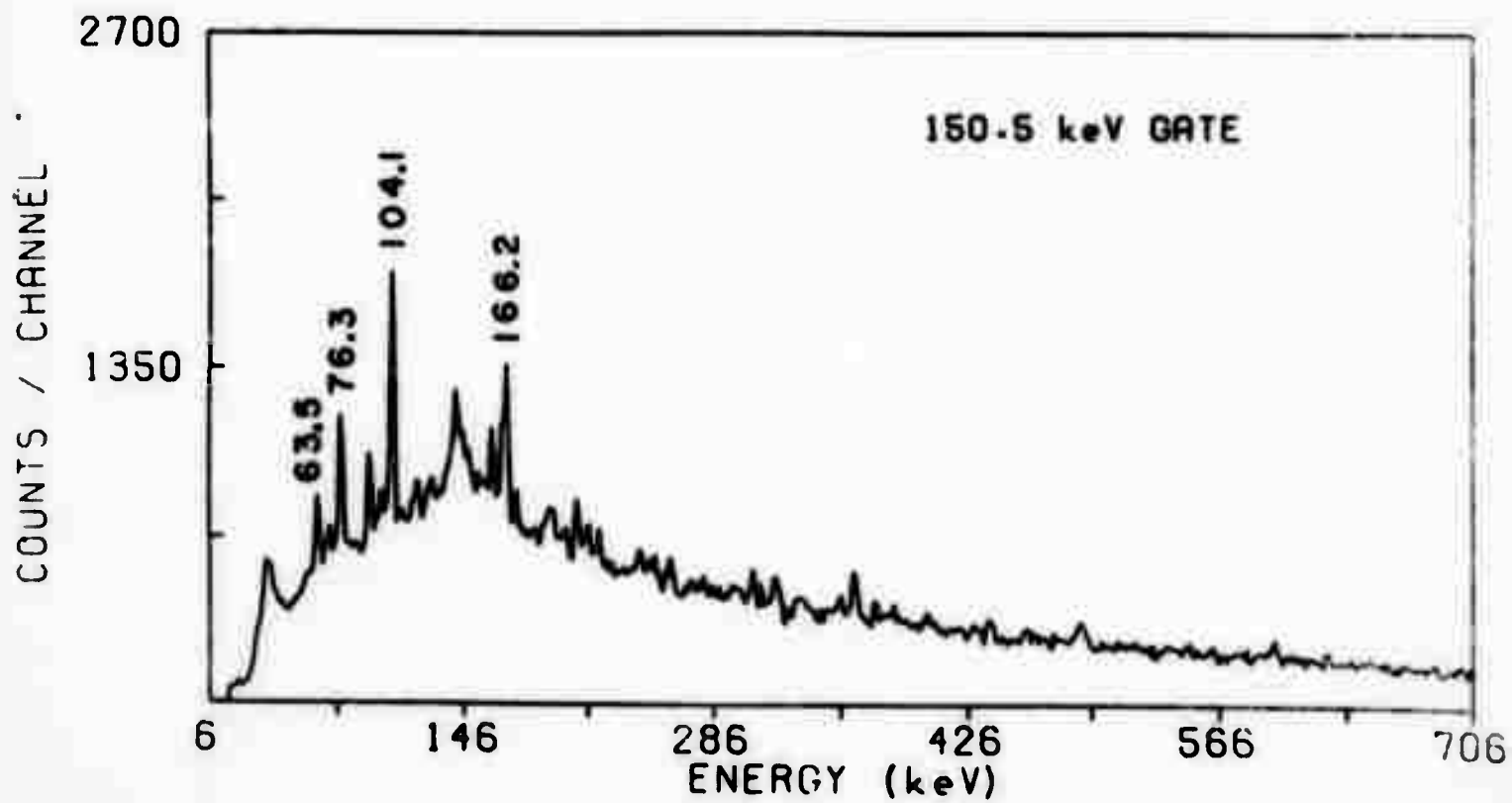
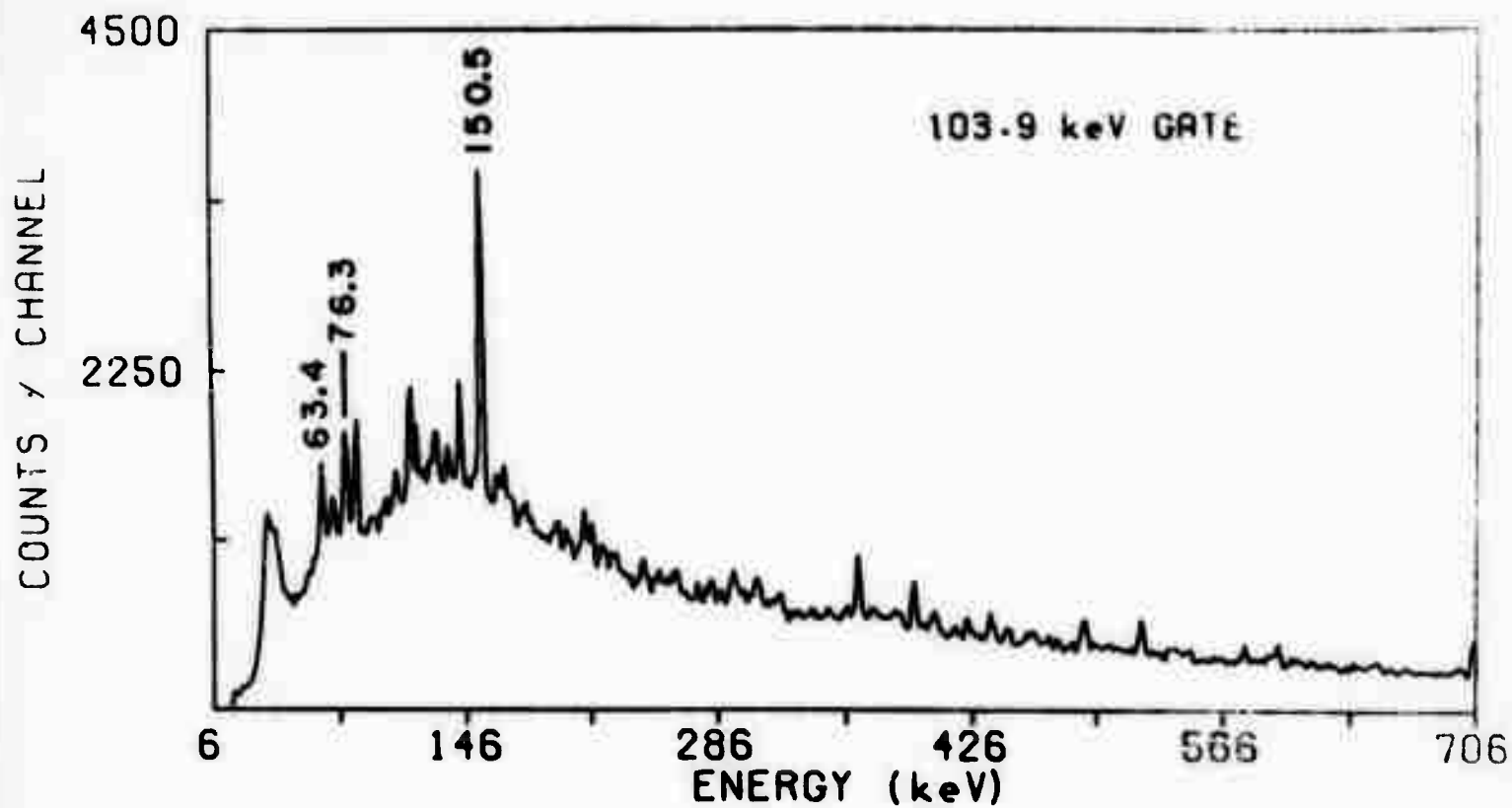




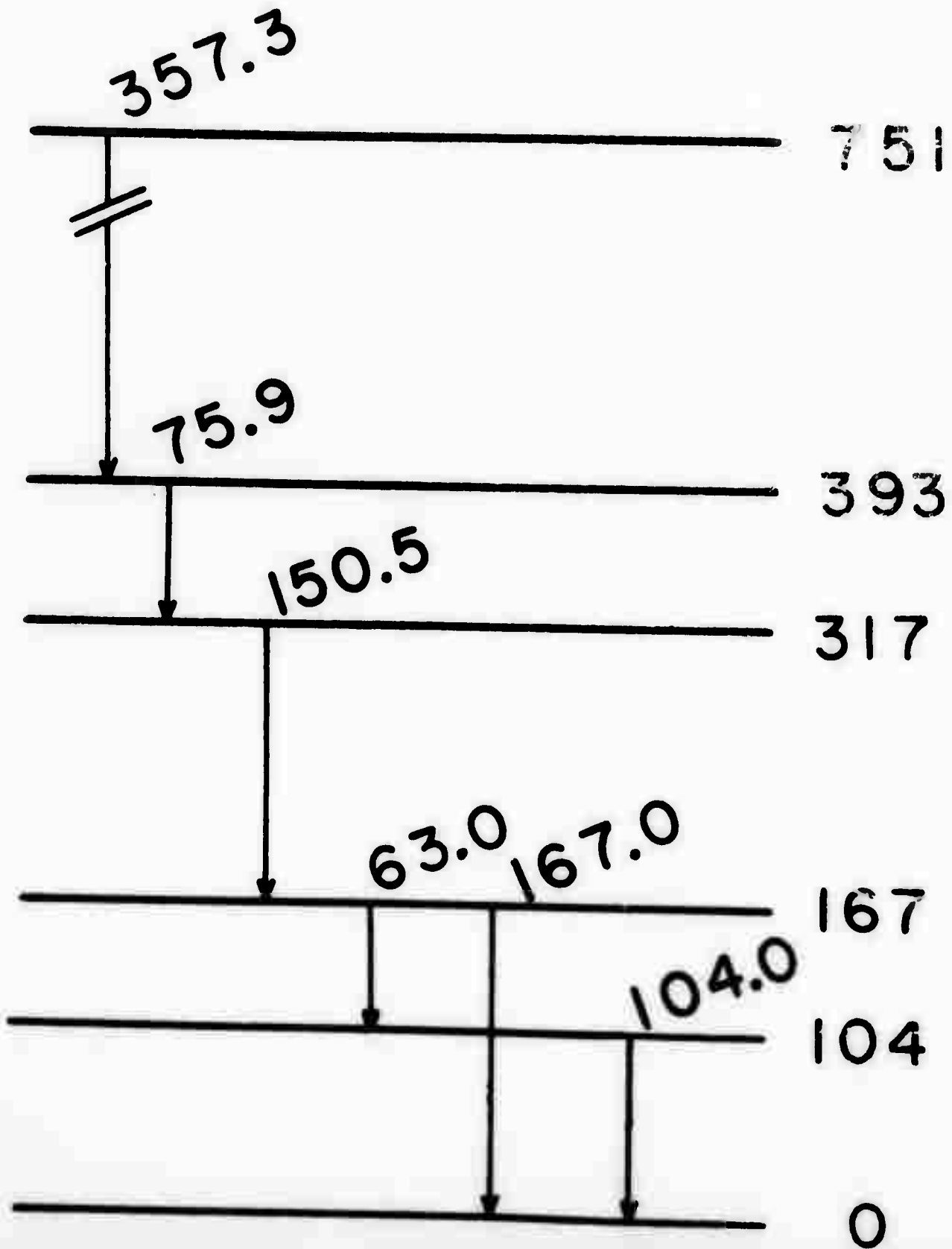


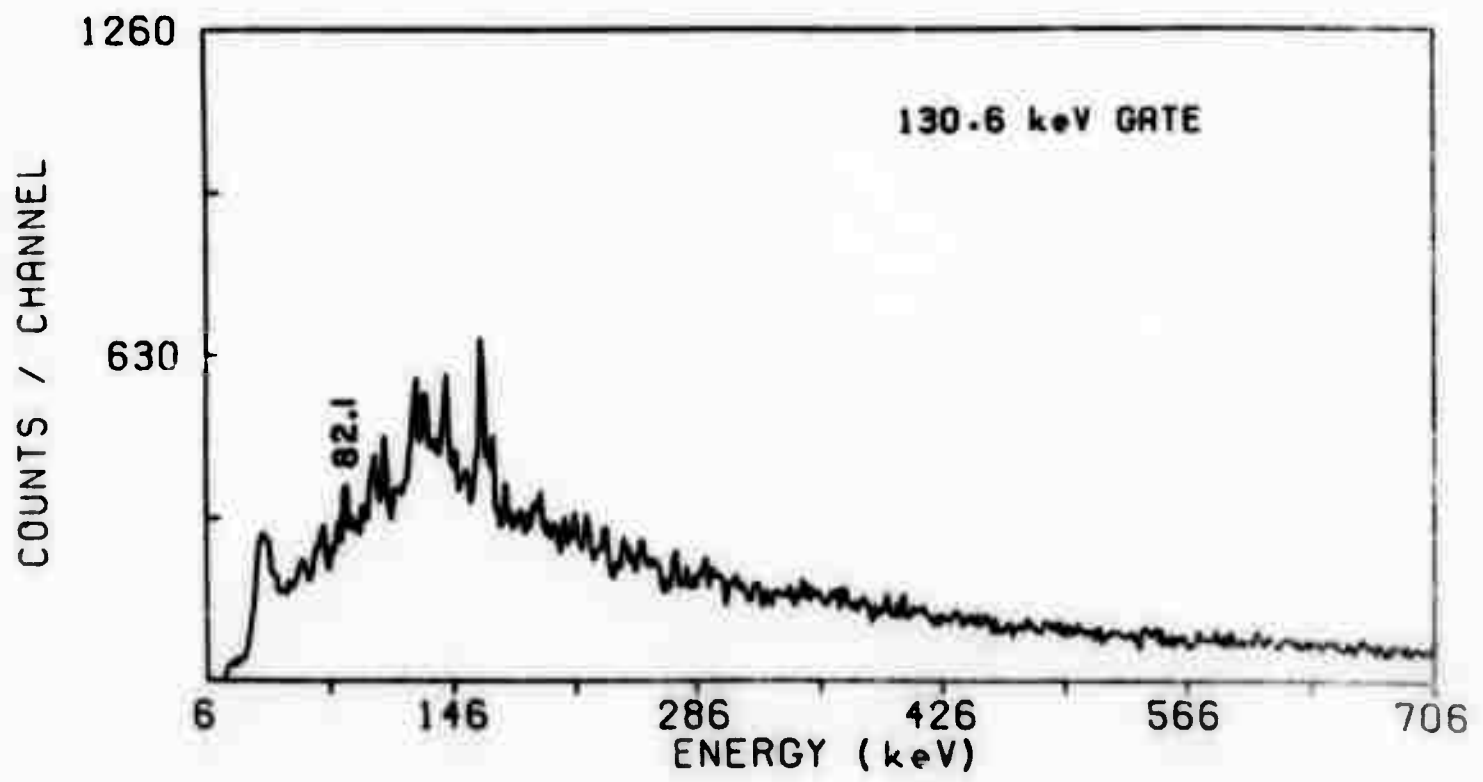
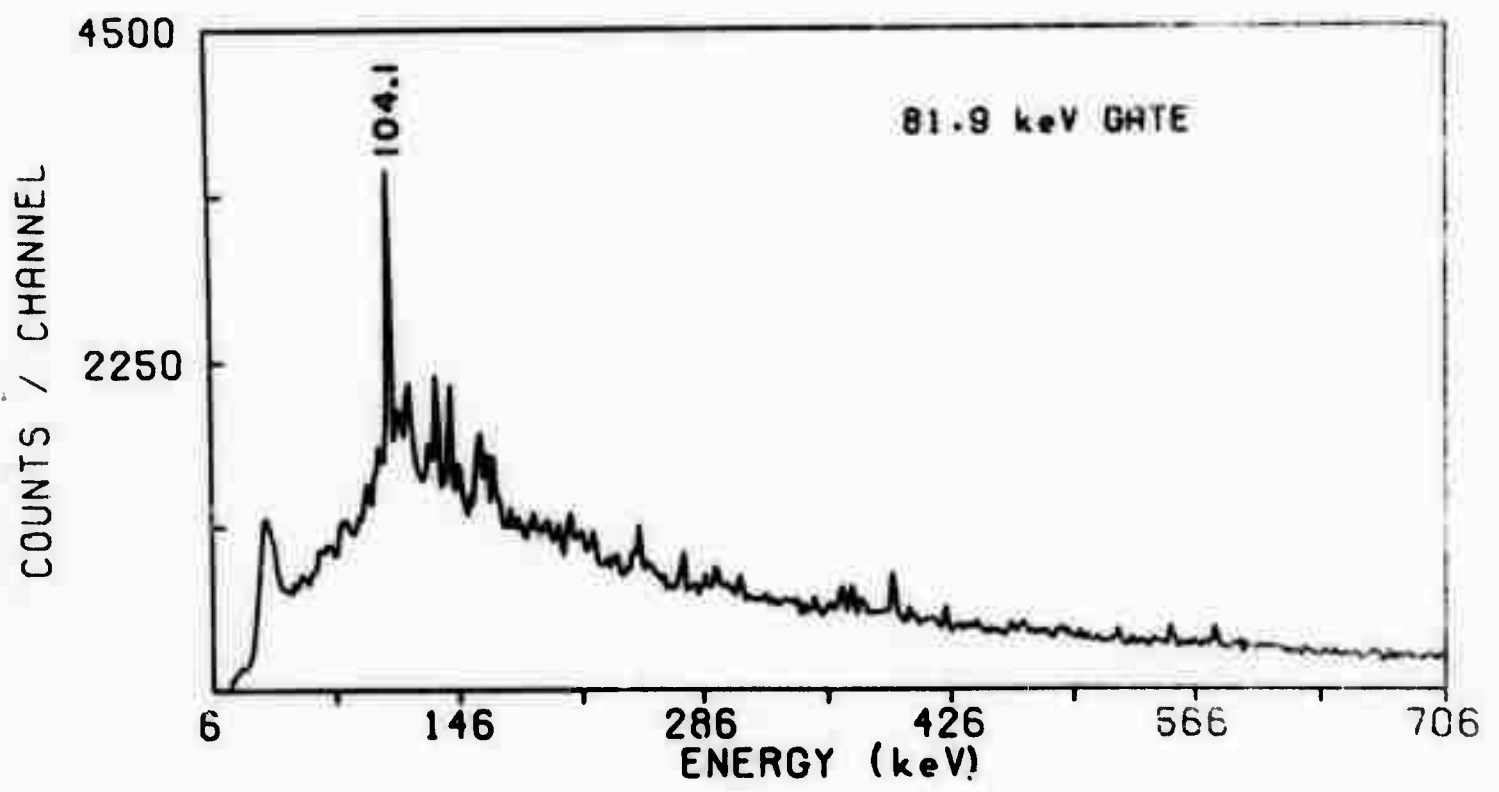
$^{109}\text{Ru}$ 





# III Ru





$^{146}\text{La}$

